BOSTON UNIVERSITY

EE529 Fall 2022

Greening and Surface Temperatures
Special Lecture
Nov-15-2022

Chi Chen
Lawrence Berkeley National Laboratory & UC Berkeley

Outline

1. Response of vegetation growth to temperature
    - Trend
    - Interannual variation
    - Seasonality and Timing
    - CO_2 : physiological and radiative effects
2. Impact of Earth greening on temperature
    - Statistical approach
    - Modeling approach
    - Data & processed-based model fusion approach

The important role of terrestrial vegetation

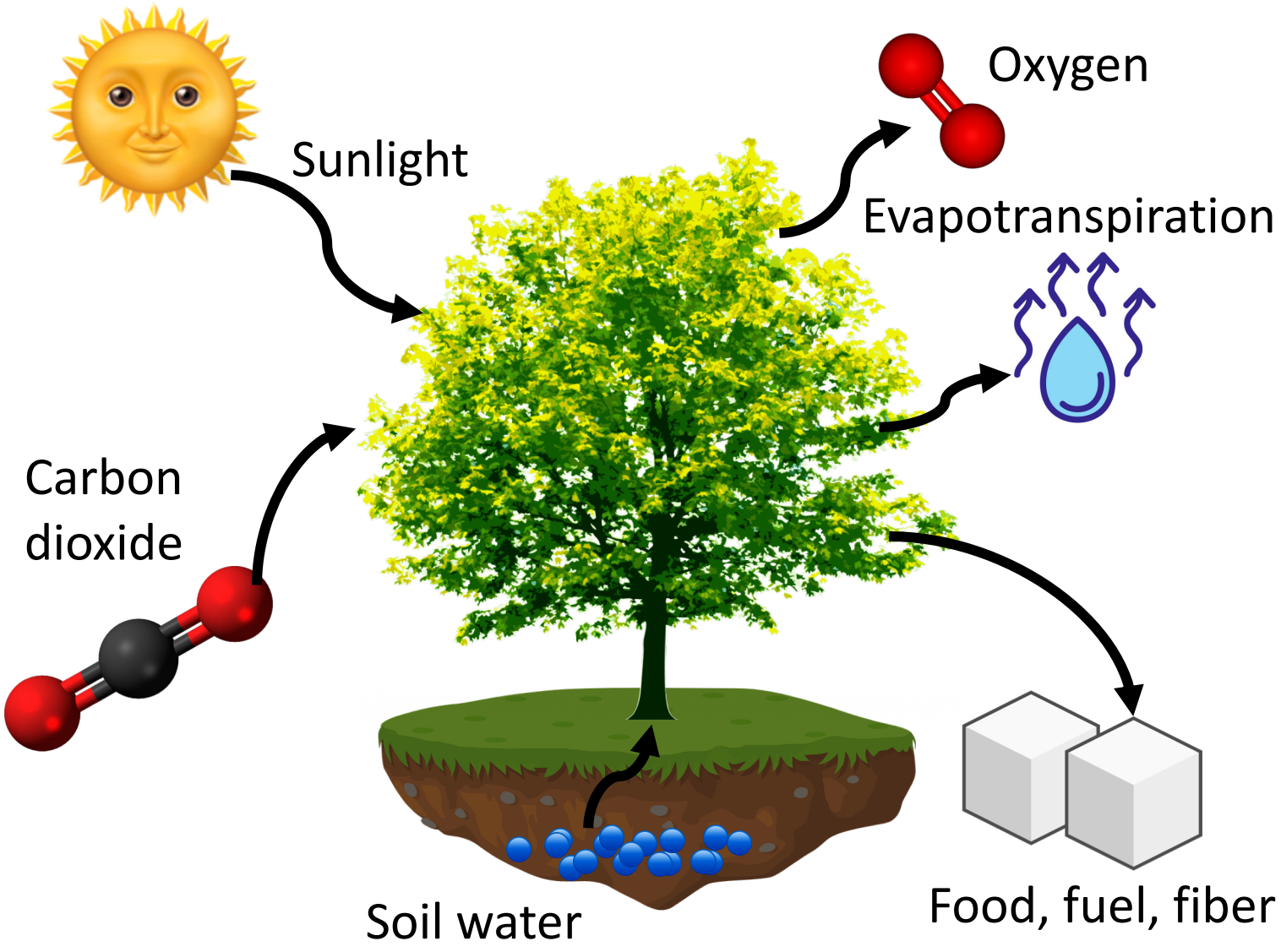

Photosynthesis generates the largest carbon flux in land-atmosphere interactions.

Essential resources limiting vegetation growth

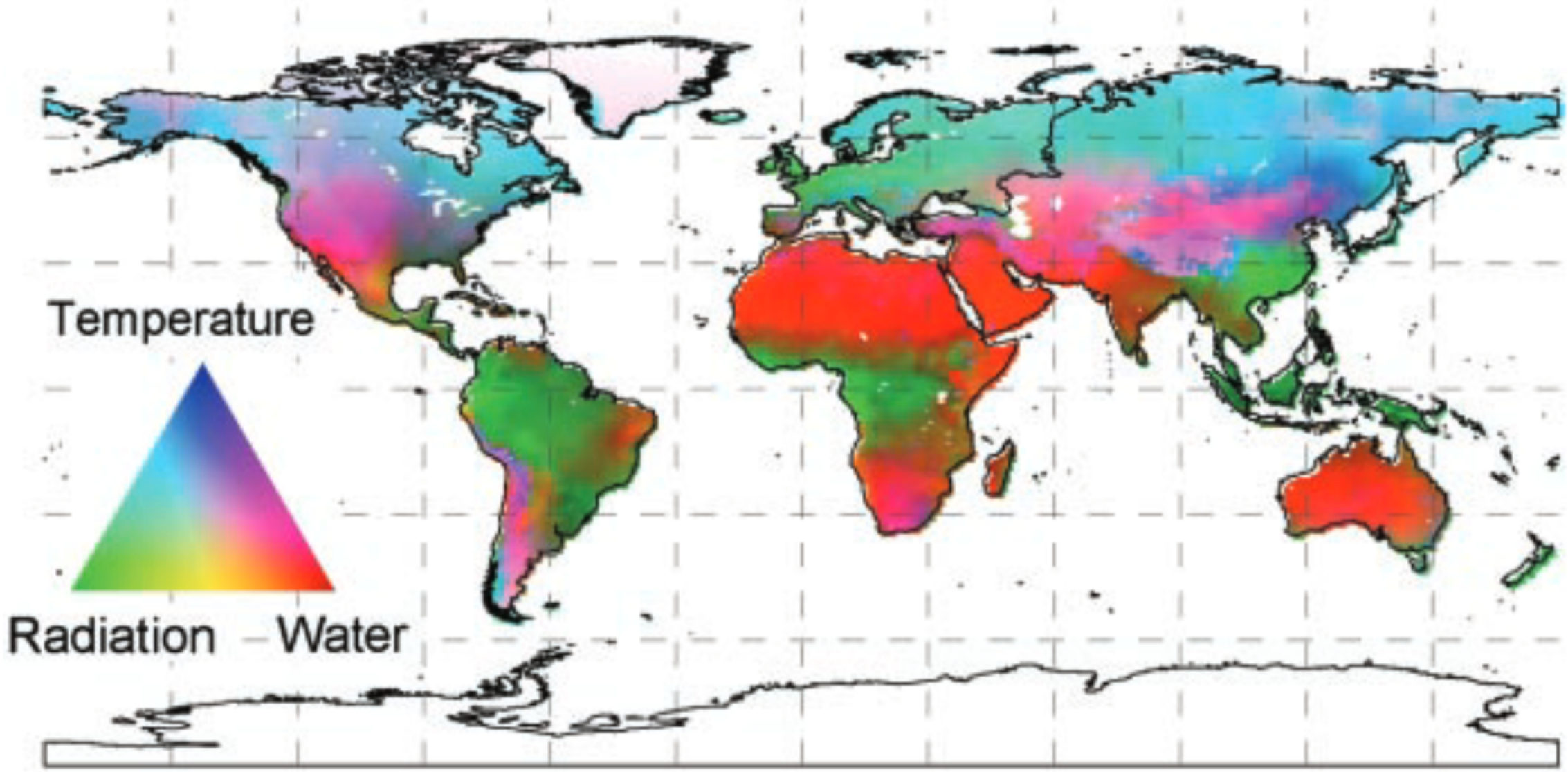

Nemani et al. (2002), *Science*

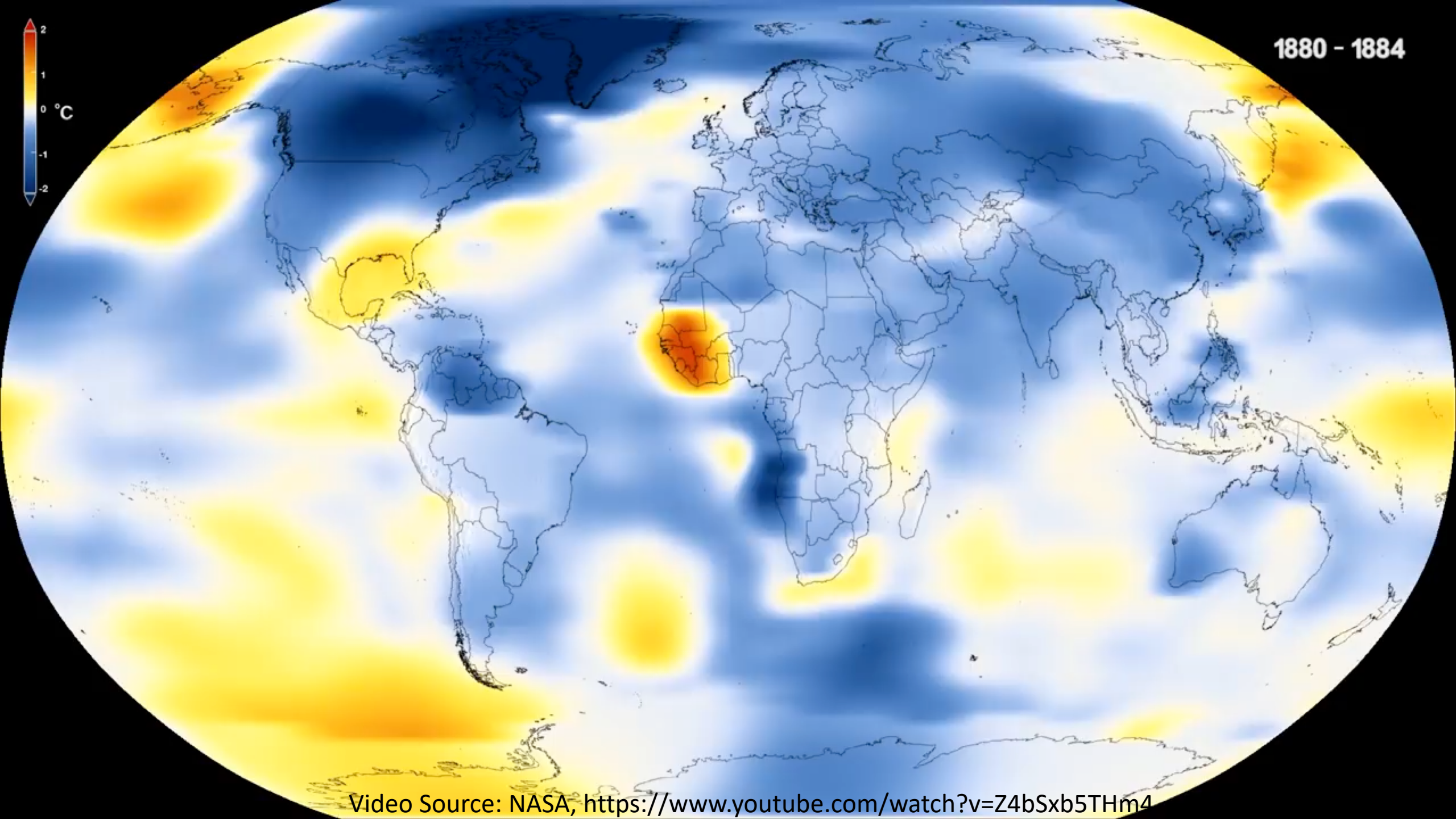

Video Source: NASA, https://www.youtube.com/watch?v=Z4bSxb5THm4

Interactions between climate change and vegetation

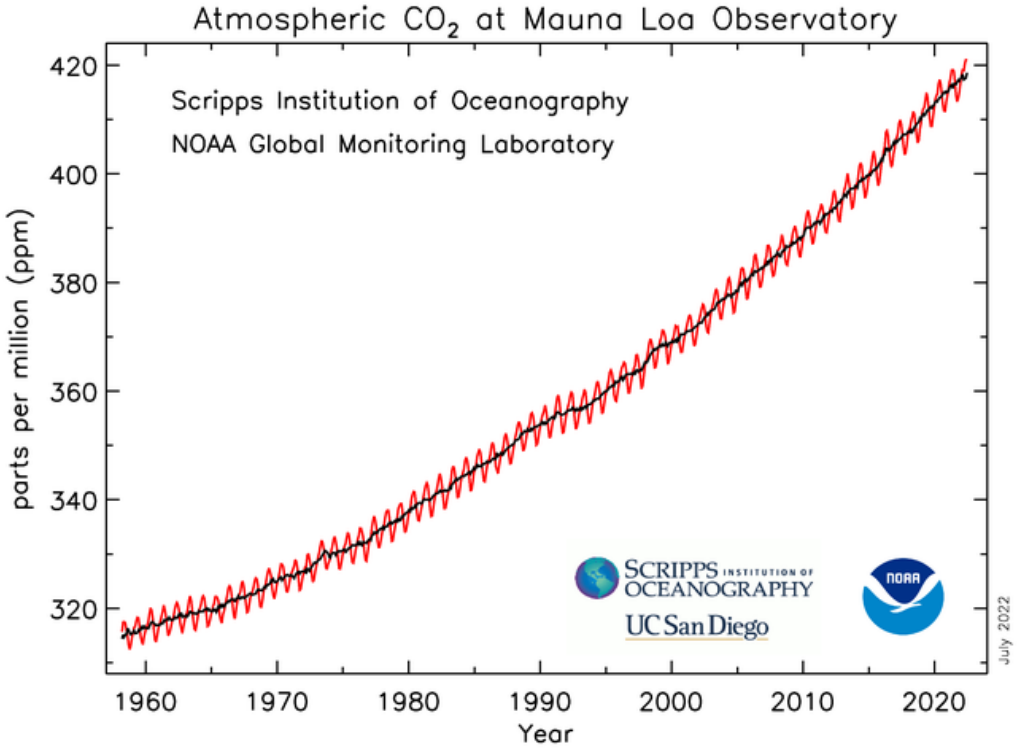

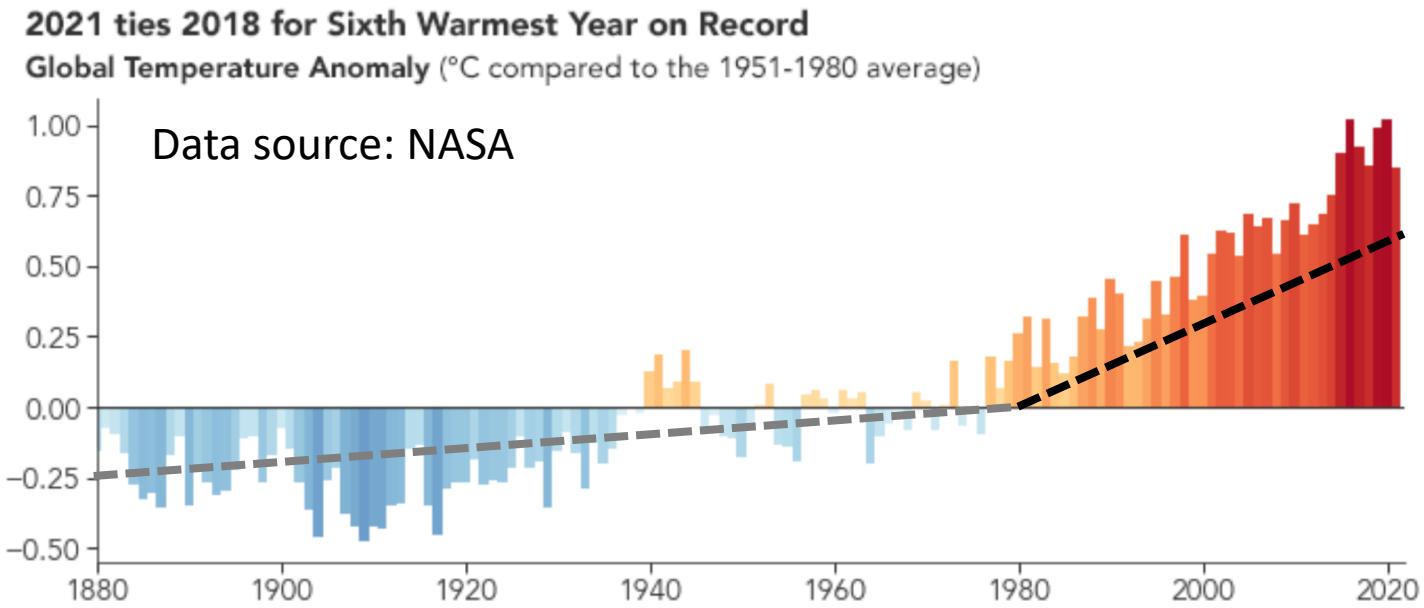

Increasing atmospheric CO_2 (421 ppm in June 2022)

- 50% more w.r.t pre-industrial time (278 ppm in 1750)

Global warming

- Speed doubled since satellite era (1980s)

How does temperature affect vegetation growth?

Earth greening and warming in T_a

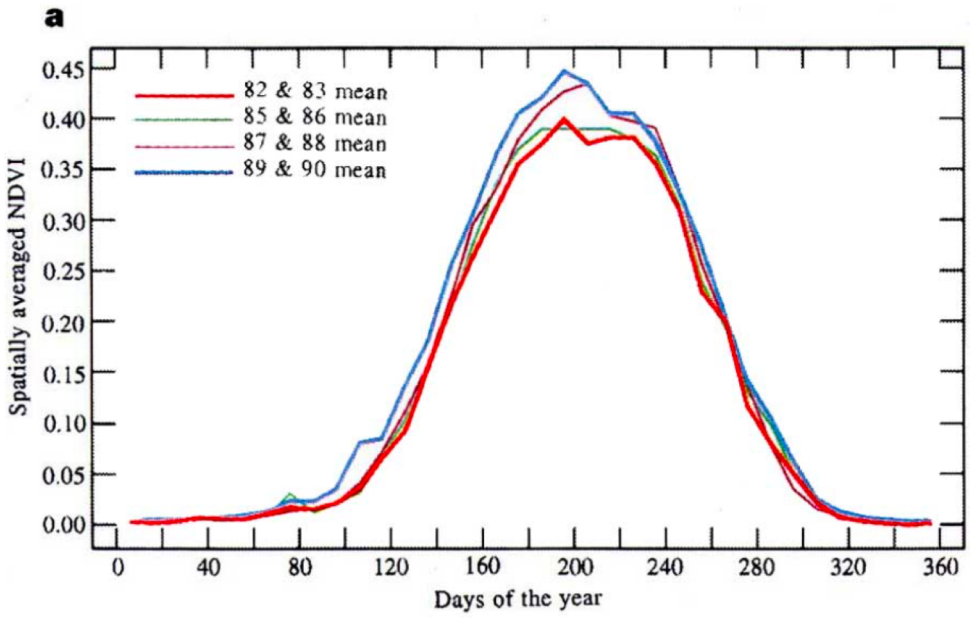

Myneni et al, 1997, Nature

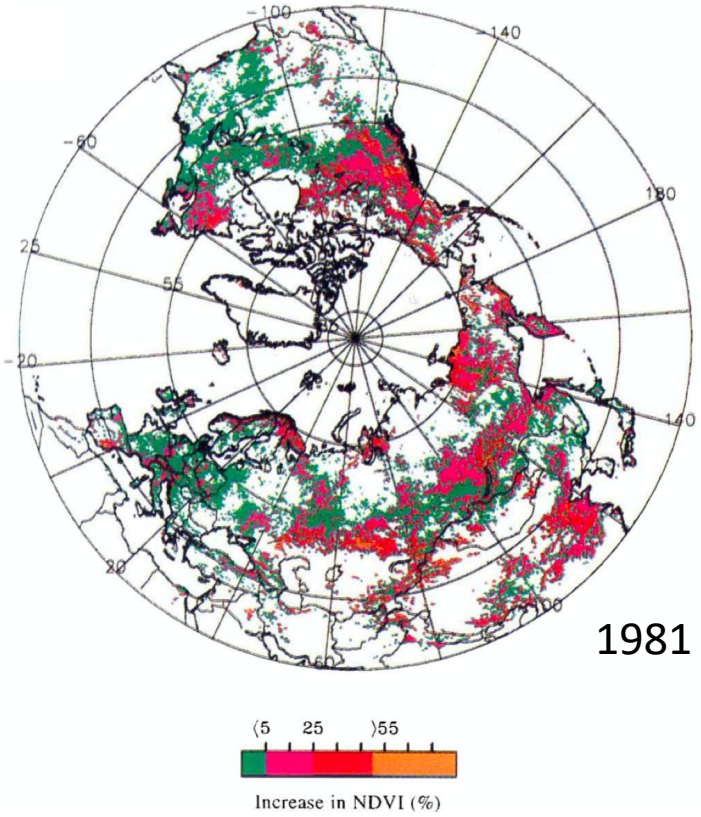

Northern high-latitude greening trend is associated with increased near-surface air temperature, especially in the early spring.

Vegetation greenness Interannual variation

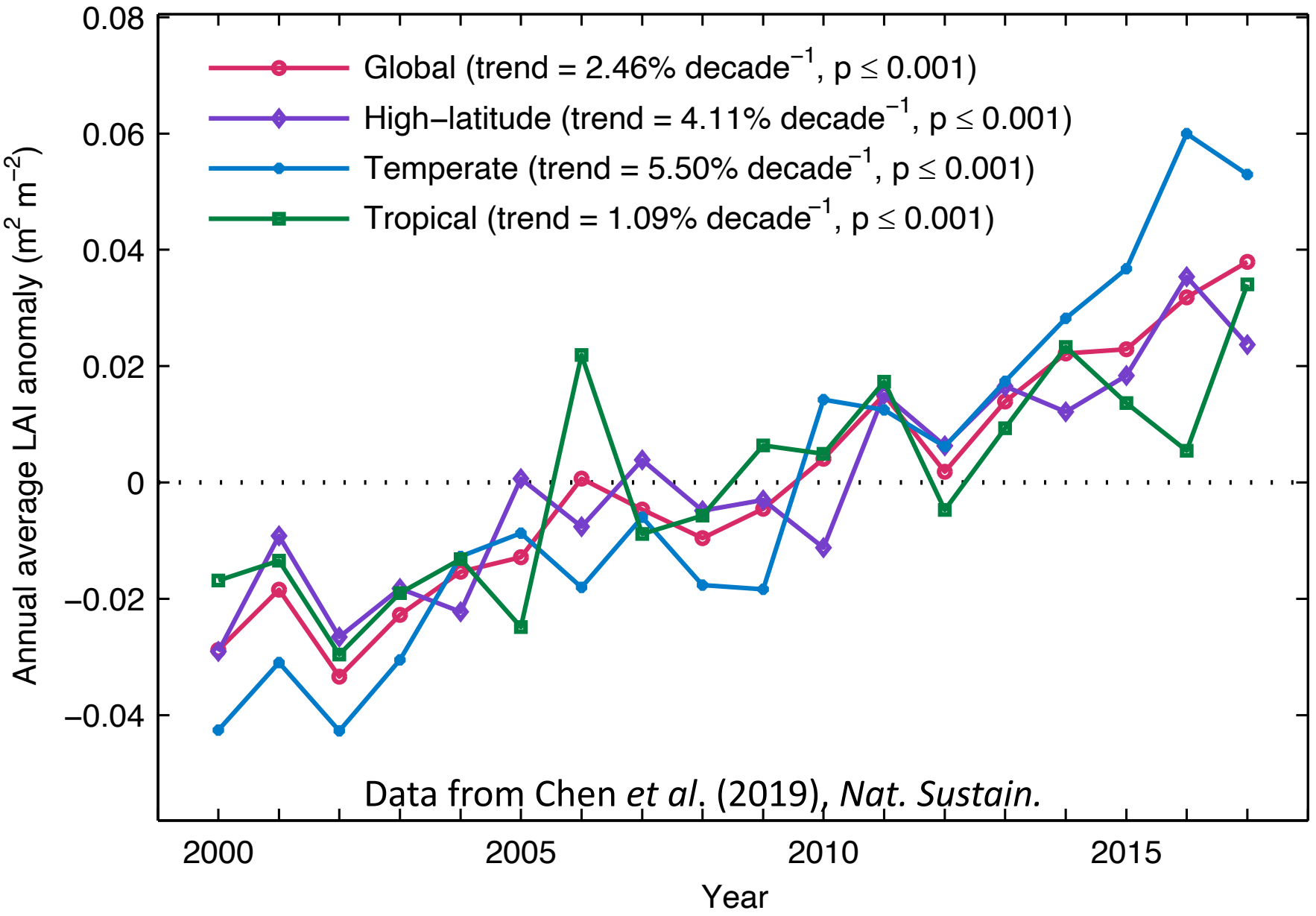

Interannual variation of greenness and T_a

$$NDVI_{sit} = \alpha_i + \sum_{s=0}^{-2} (\beta_{si1} Temp_{sit} + \beta_{si2} Temp_{sit}^2 + \beta_{si3} Prec_{sit} + \beta_{si4} Prec_{sit}^2) + \beta_{si5} SZA_{sit} + \beta_{si6} AOD_{sit} + \varepsilon_{sit}.$$

[1] This paper analyzes the relation between satellite-based measures of vegetation greenness and climate by land cover type at a regional scale (2° × 2° grid boxes) between 1982 and 1999. We use the normalized difference vegetation index (NDVI) from the Global Inventory Monitoring and Modeling Studies (GIMMS) data set to quantify climate-induced changes in terrestrial vegetation. Climatic conditions are represented with monthly data for land surface air temperature and precipitation. The relation between NDVI and the climate variables is represented using a quadratic specification, which is consistent with the notion of a physiological optimum. The effects of spatial heterogeneity and unobserved variables are estimated with specifications and statistical techniques that allow coefficients to vary among grid boxes. Using this methodology, we are able to estimate statistically meaningful relations between NDVI and climate during spring, summer, and autumn for forests between 40°N and 70°N in North America and Eurasia. Of the variables examined, changes in temperature account for the largest fraction of the change in NDVI between the early 1980s and the late 1990s. Changes in stratospheric aerosol optical depth and precipitation have a smaller effect, while artifacts associated with variations in solar zenith angle are negligible. These results indicate that temperature changes between the early 1980s and the late 1990s are responsible for much of the observed increase in satellite measures of northern forest greenness. *INDEX TERMS:* 1615 Global Change: Biogeochemical processes (4805); 1620 Global Change: Climate dynamics (3309); 1640 Global Change: Remote sensing; *KEYWORDS:* NDVI, climate, greening, temperature, statistical techniques

Temperature drives vegetation interannual variation, in particular, the boreal regions

Zhou et al, 2001, JGR

Greenness and T_a seasonalities

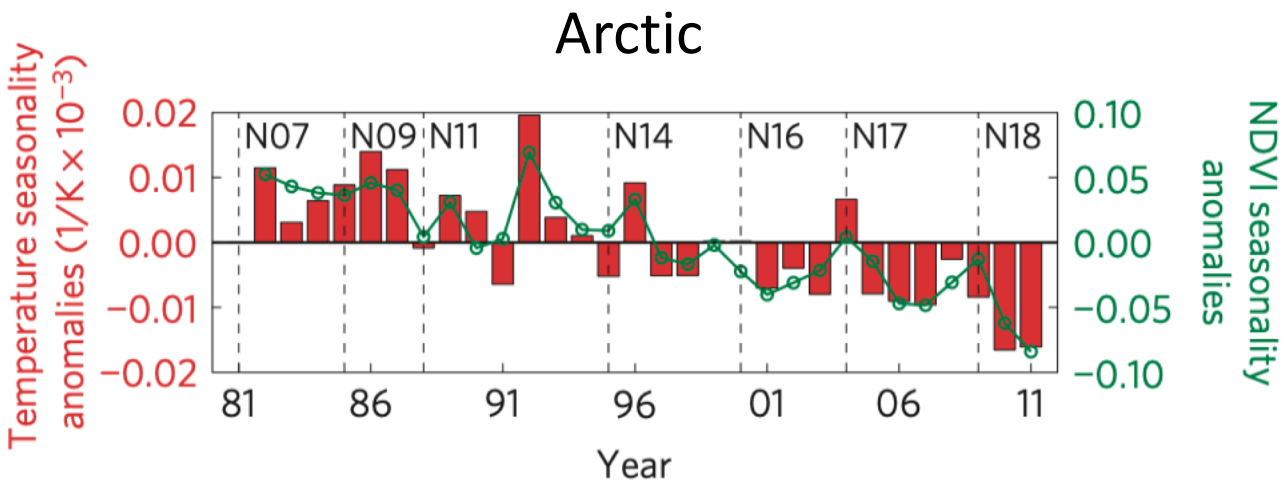

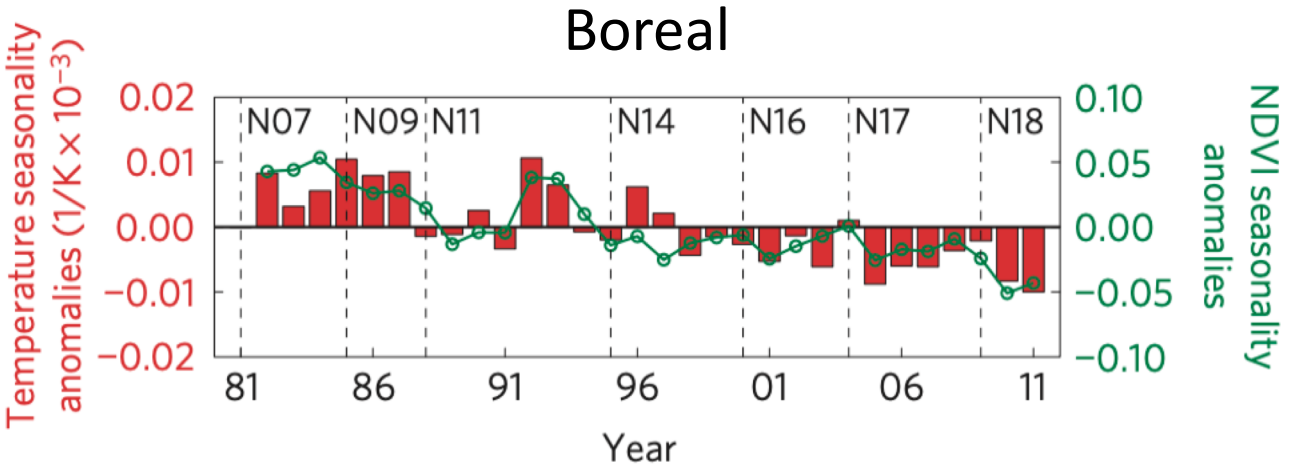

- T_a seasonality: $T_{max} - T_{min}$
- Greenness seasonality: $NDVI_{max}$ - $NDVI_{min}$

Vegetation greenness seasonality anomaly is highly correlated with the temperature seasonality anomaly.

Xu et al, 2013, Nature Climate Change

Advancement of peak vegetation productivity timing

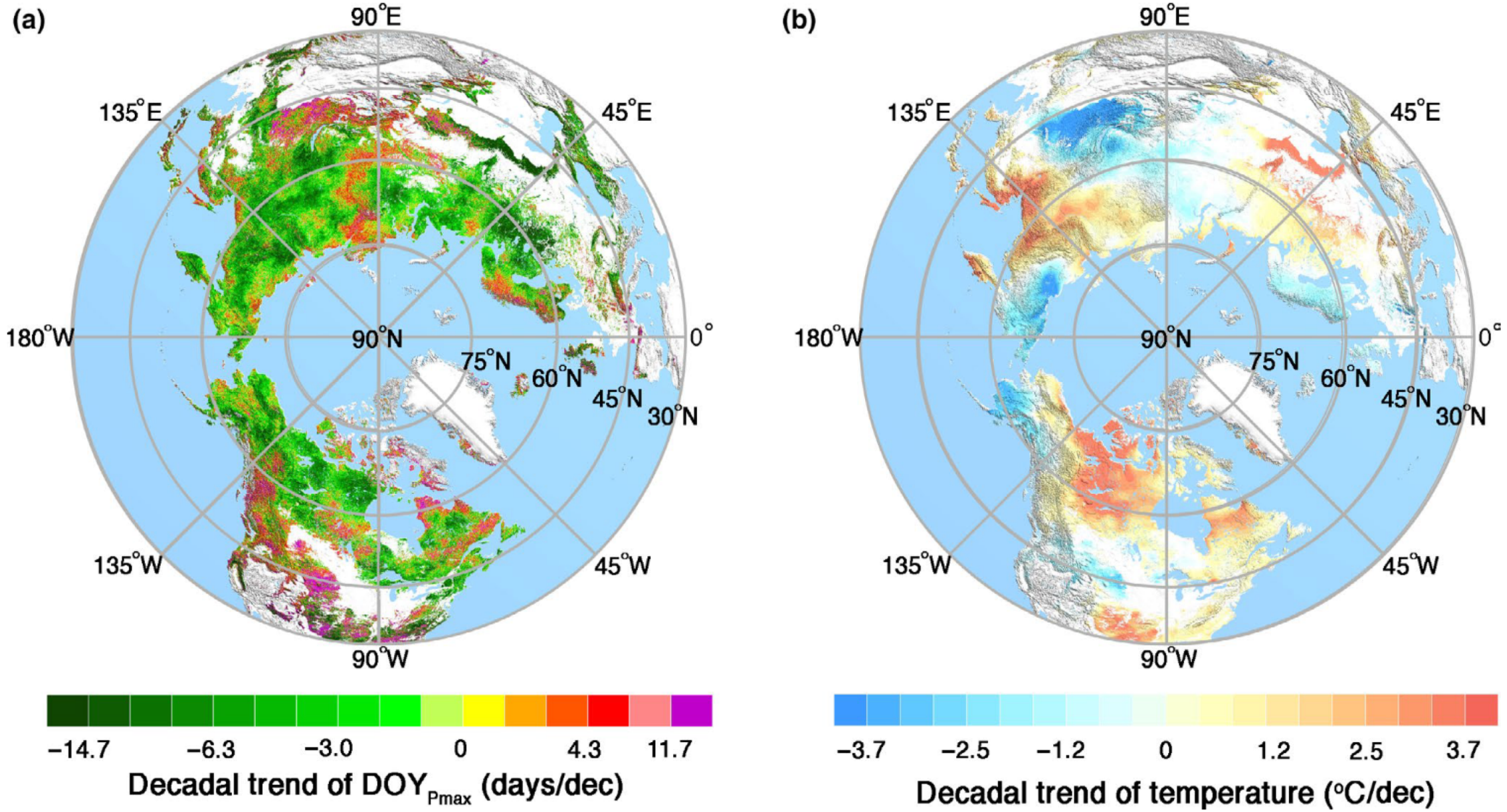

Park & Chen et al (2019)

Greenness ⇔ T_a and CO_2

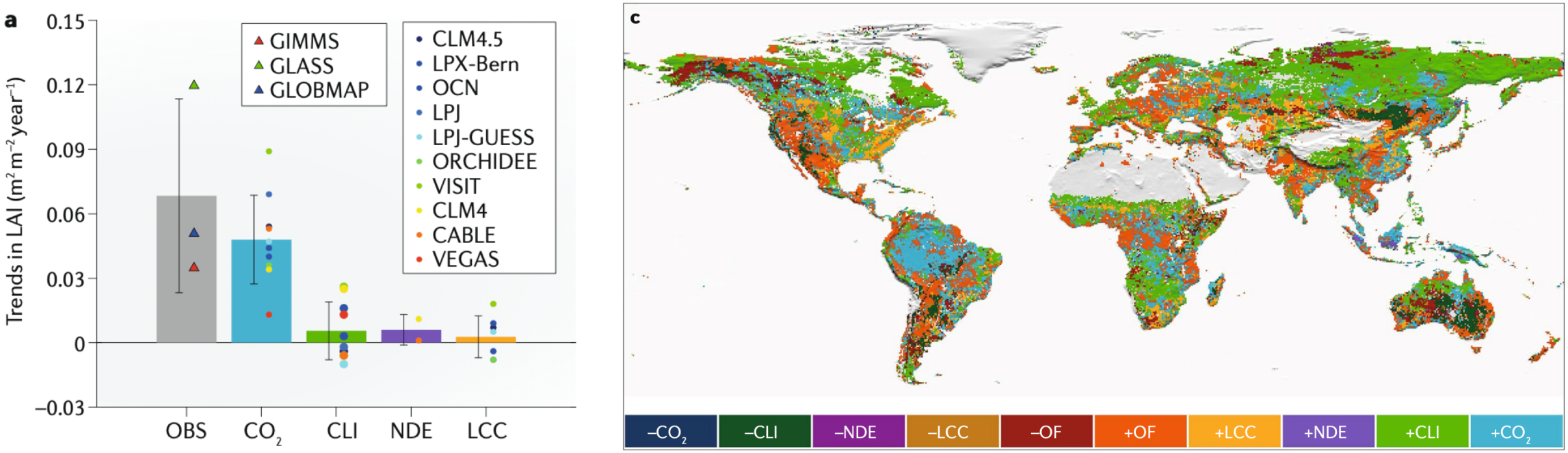

Figure credit : Zhu et al, 2016, Nature Climate Change; Piao et al, 2019, Nature Reviews for Earth & Environ.

- Model simulations suggests that CO_2 explains most of the increasing trend in LAI in attribution analysis.

- CLI (i.e., temperature, precipitation) is the dominant factor in controlling LAI anomalies.

Historical relationship between T_a and CO_2

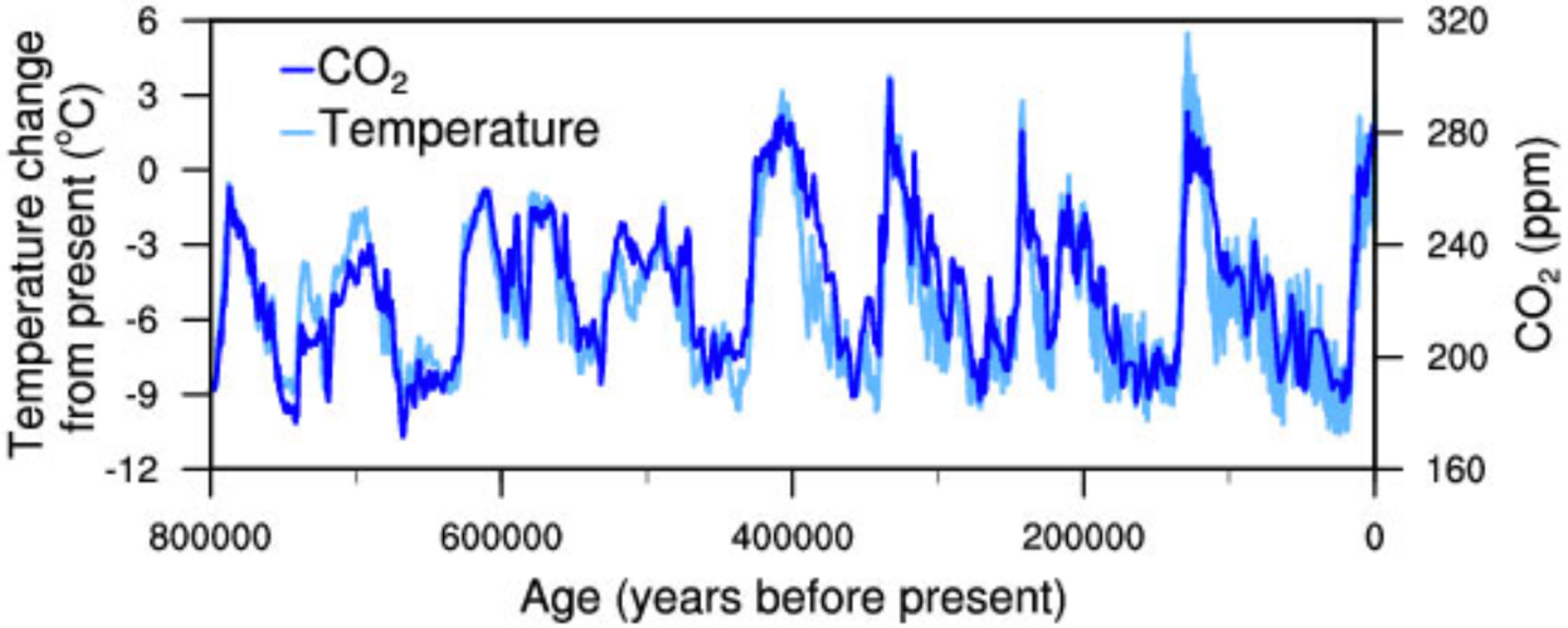

Temperature change (light blue) and carbon dioxide change (dark blue) measured from the EPICA Dome C ice core in Antarctica (Jouzel et al. 2007; Lüthi et al. 2008).

Satellite-derived CO_2 fertilization effect (CFE)

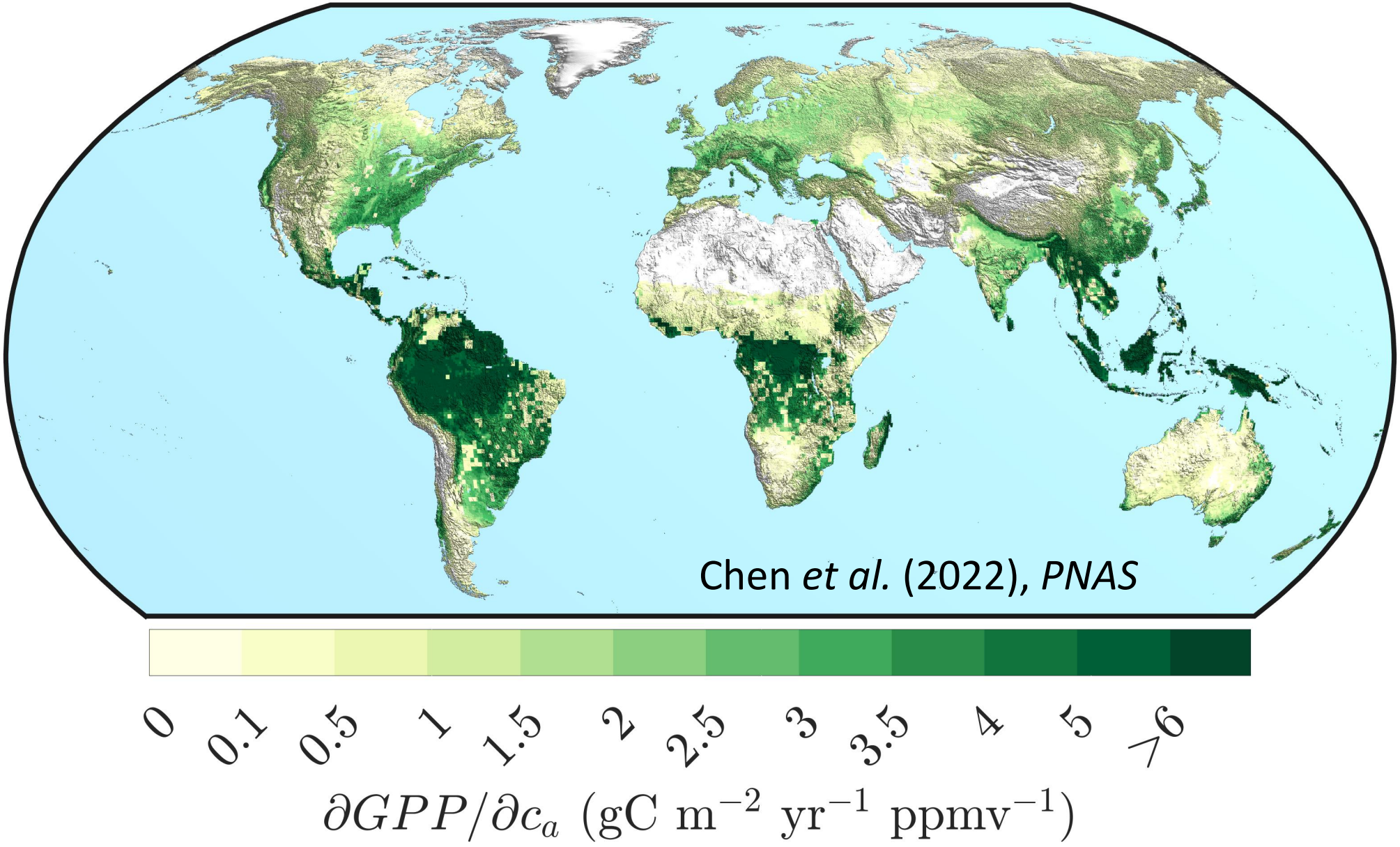

Global mean $\frac{\partial GPP}{\partial c_a}$ = 2.02 gC $m^{-2}yr^{-1}$ ppm^{-1}

CO_2-induced GPP trend= 4.1% GPP $decade^{-1}$

CFE is strongest in tropical forests

Site analysis of GPP sensitivity to factors

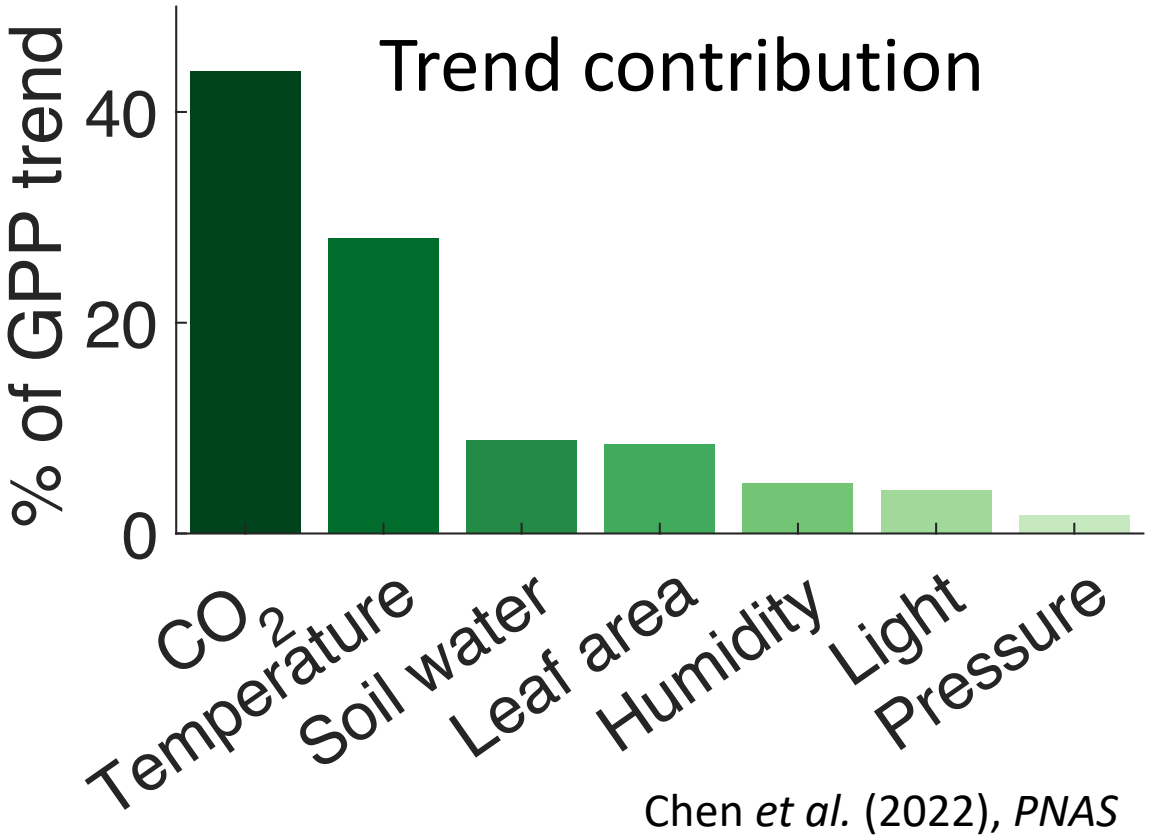

Chen *et al.* (2022), *PNAS*

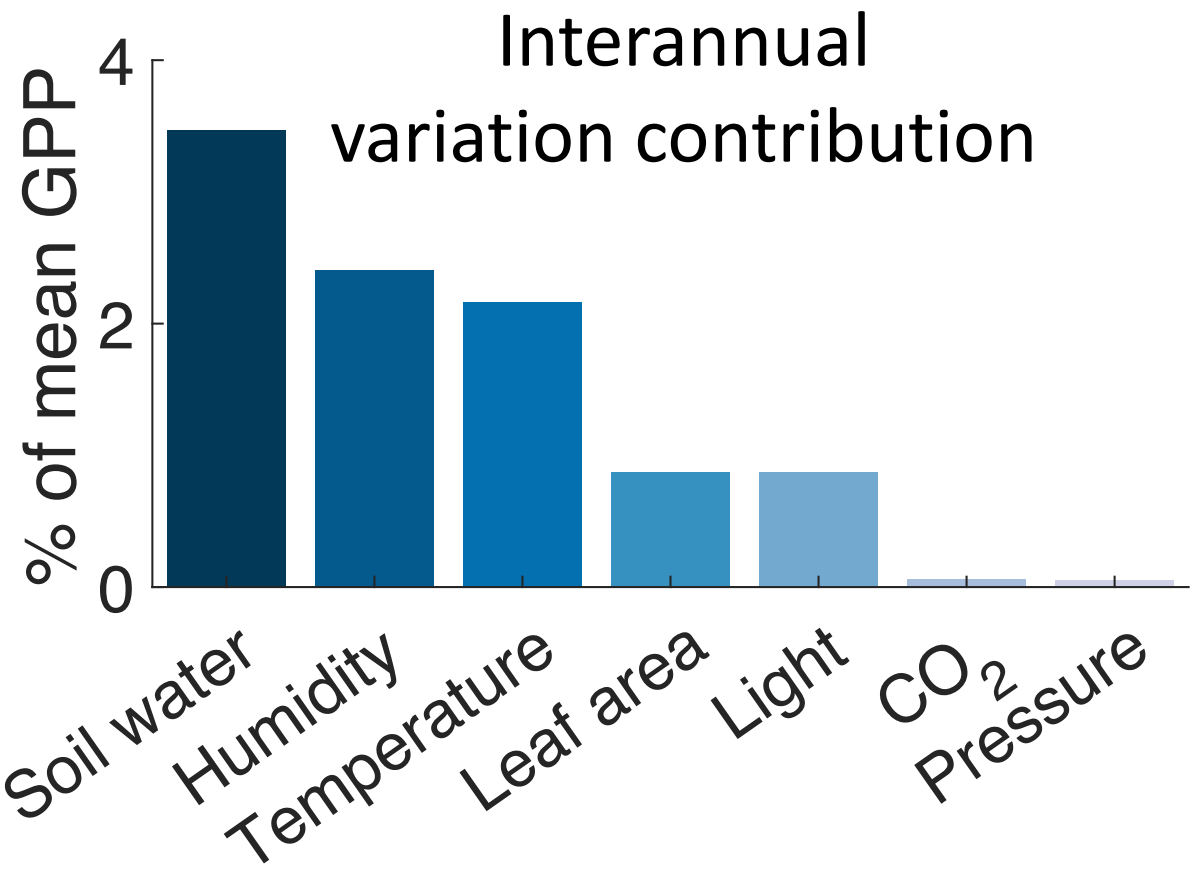

T_a contributes over 28% to the GPP trend

Ability of each factor (X) to cause GPP IAV

- $\frac{\partial GPP}{\partial X} \times Std_X \div GPP_{mean}$

Breakdown for the temperature pathway

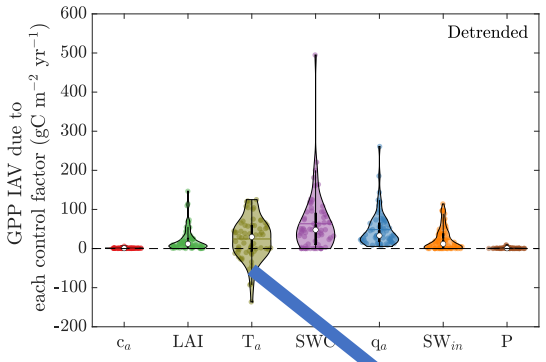

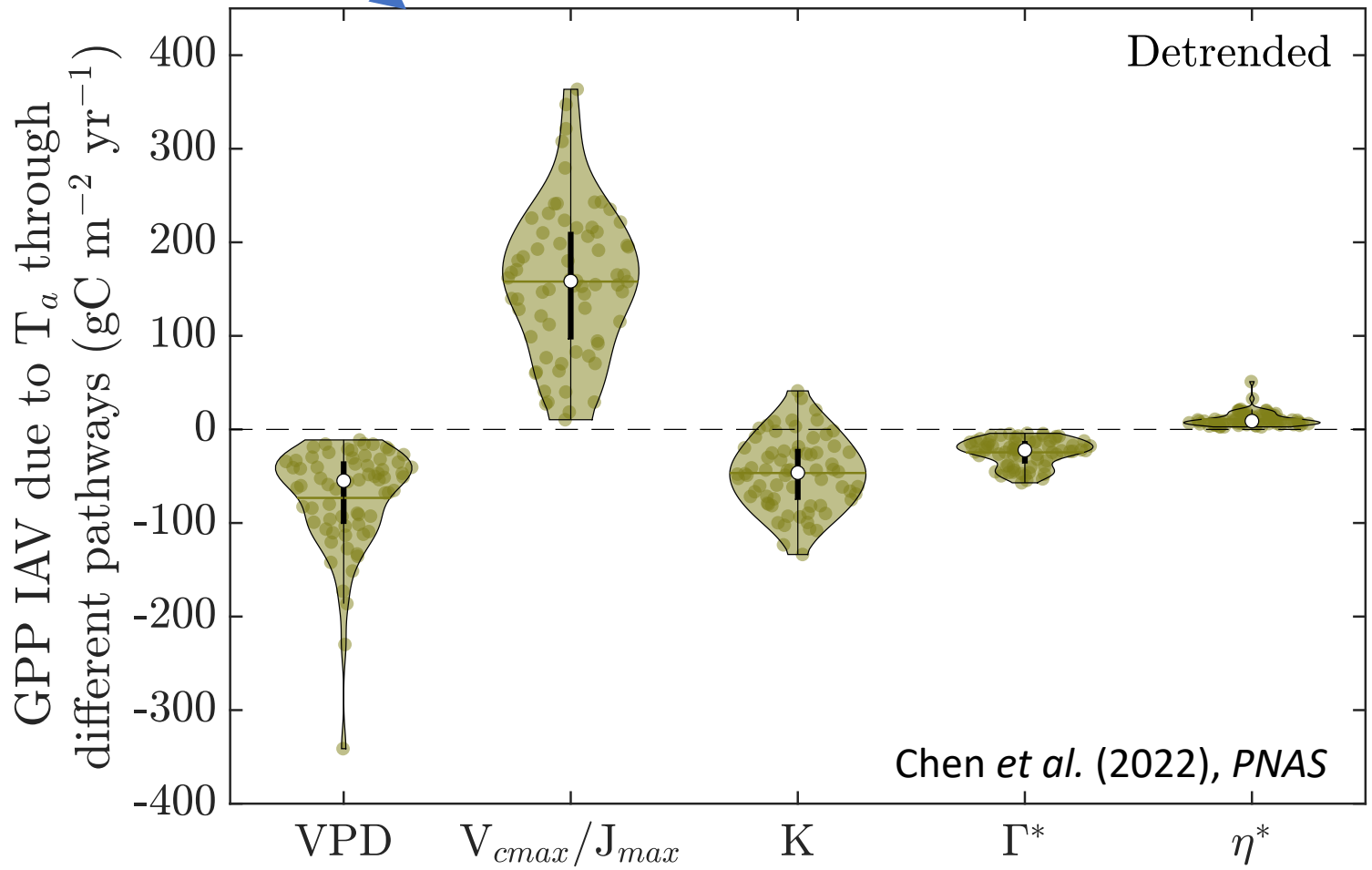

Complex processes associated with temperature

Temperature effect on vegetation productivity

Temperature can affect multiple processes of vegetation growth. Greening observed from satellite data is only one aspect of the complex vegetation system.

At short terms, temperature can

- increase the enzyme energetics during the photochemical processes of carbon fixation [Farquhar et al (1980), Kattge et al (2007)].
- influence plant optimization to its growing environment, such as by regulating stomatal conductance and leaf CO_2 concentration [Chen et al., 2022].
  - "Quick legacy" effect of enzyme energetics
  - VPD
- regulates the ecosystem respirations [Reich et al (2016), Keenan et al (2017)]
- …

Long-term scales: adaptation to the growing environment, such as structural change, species shifting, photosynthetic traits change, respiration acclimation [e.g., Wang et al. (2020)].

Evolutionary scales…

Greening in the MODIS era (2000-present)

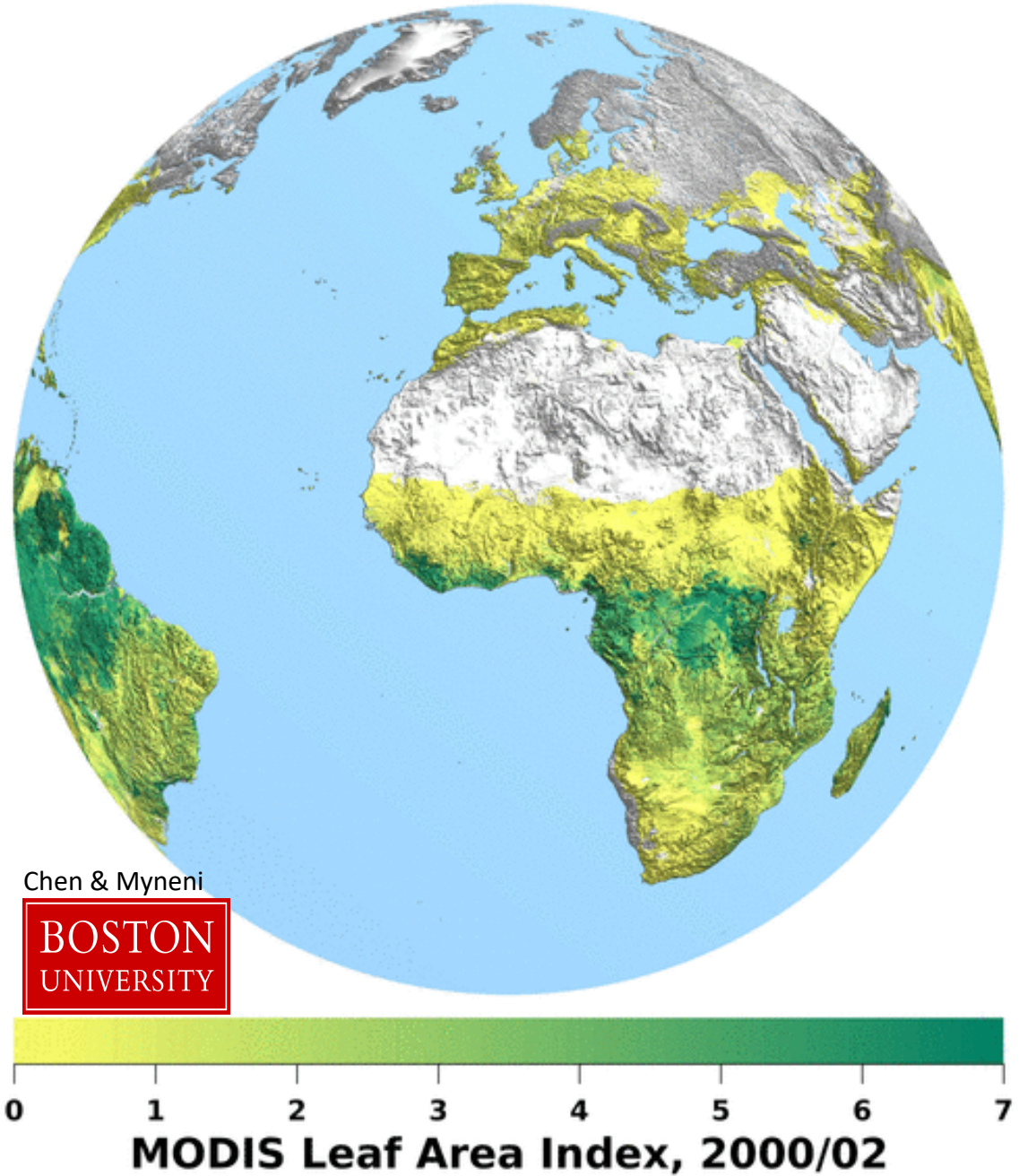

The most up-to-date, consistent and detailed quality-controlled leaf area index data from satellites.

Hotspots of greening areas

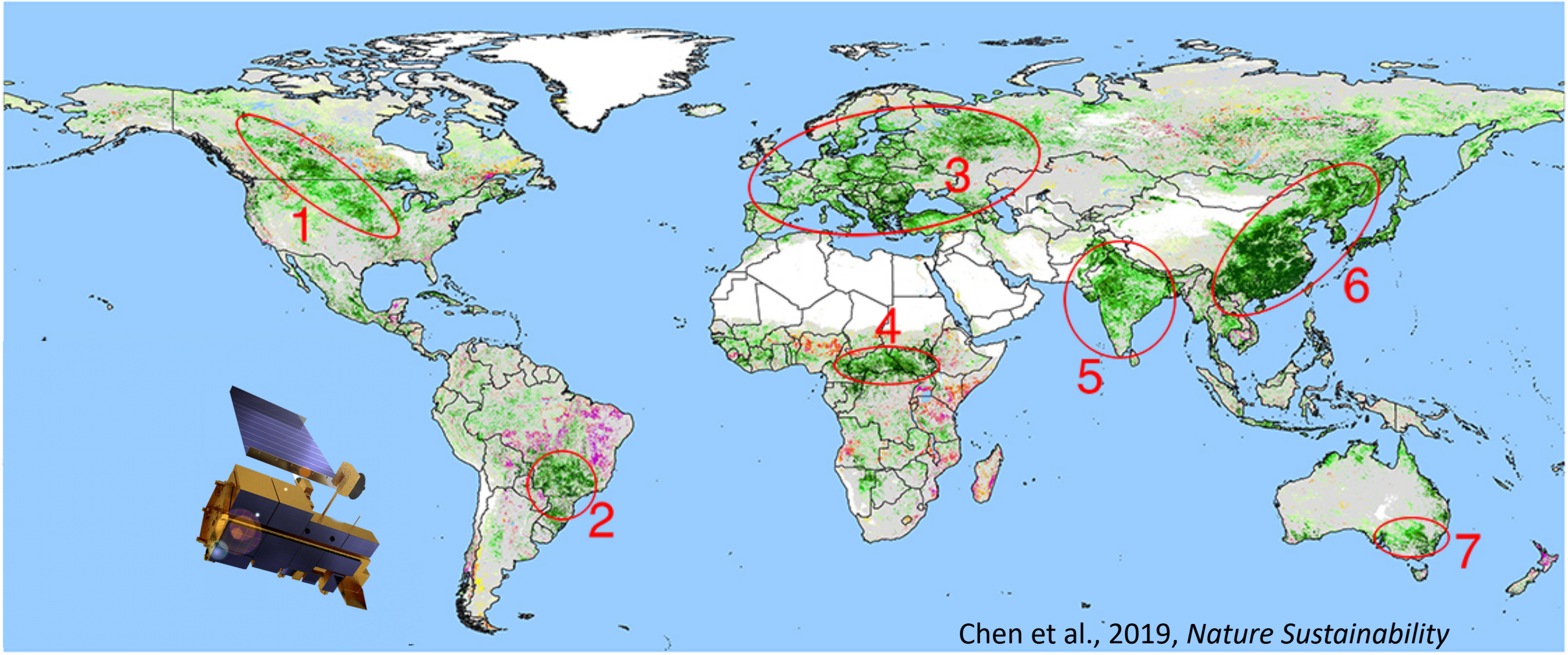

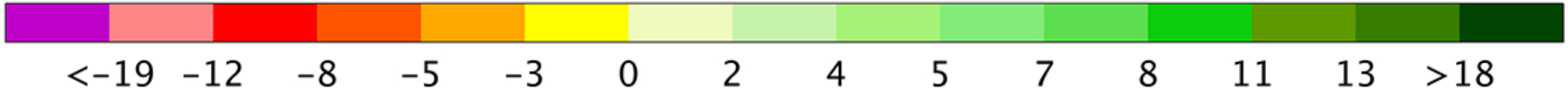

Trend in annual average LAI ($10^{-2}m^2m^{-2}decade^{-1}$, $p < 0.1$)

Croplands contribute 1/3 of the global greening

Contribution (%) to the net increase in leaf area

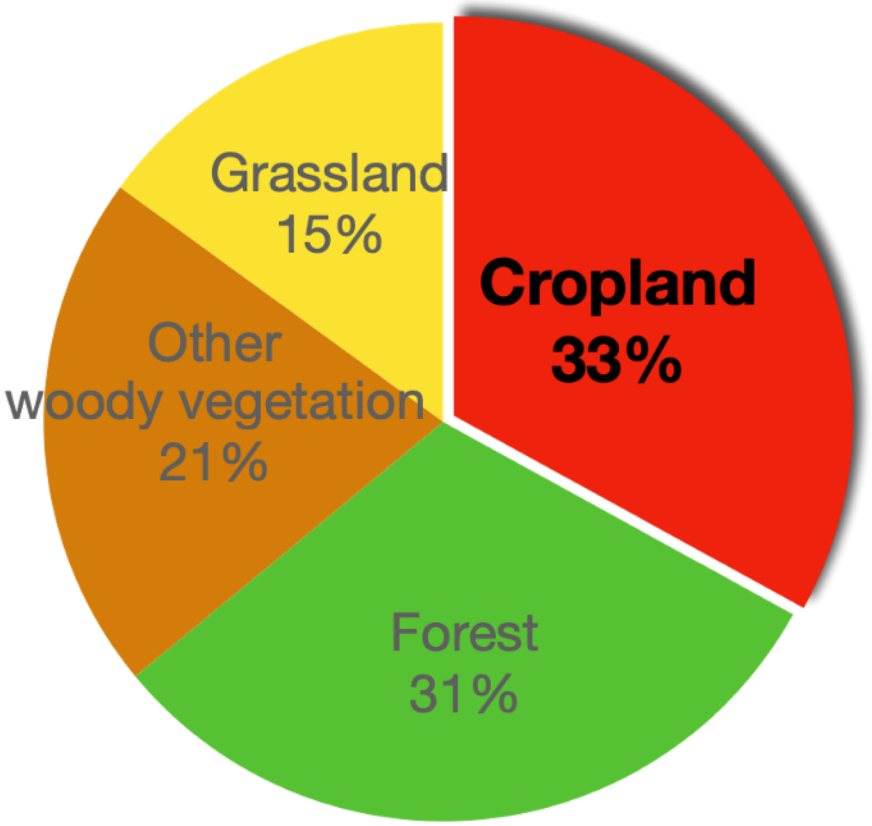

Chen *et al*. (2019), *Nat. Sustain.*

Croplands contribute 1/3 of the global greening

Contribution (%) to the net increase in leaf area

UN FAO statistics

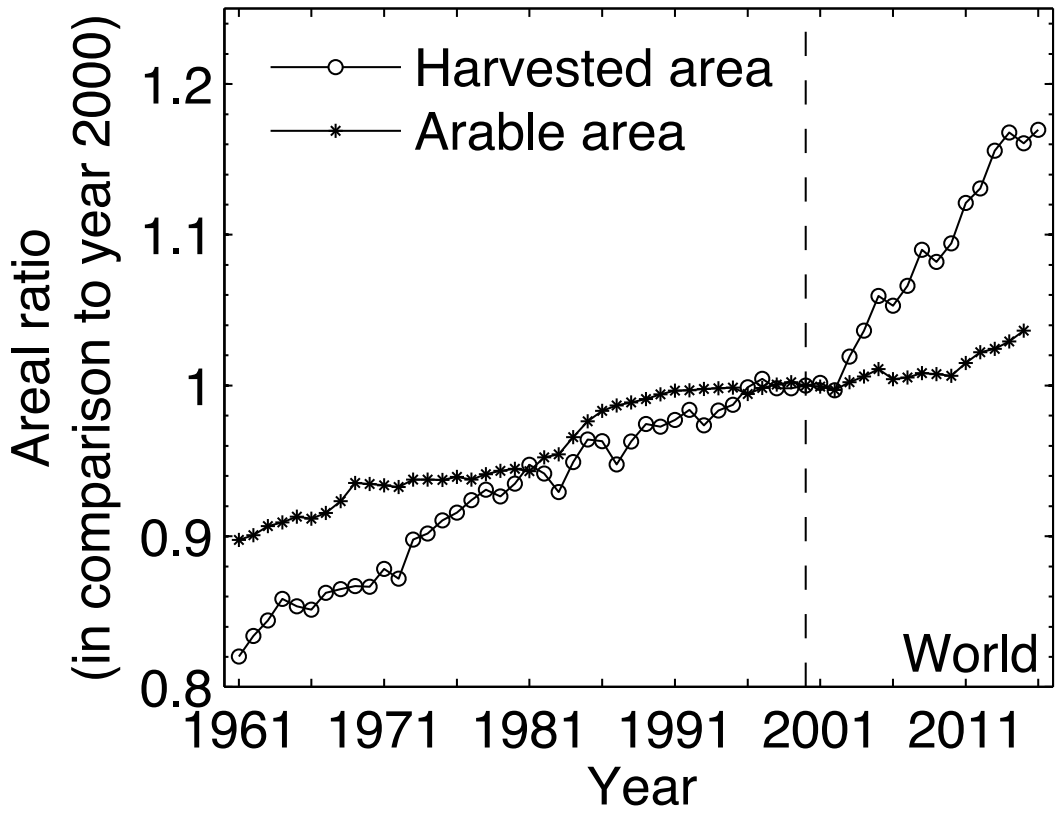

- **Land-use management**: Harvested area at the global scale grew four times faster than the arable area since 2000
- Agricultural dry matter change: Brazil (76% dec^{-1}), India (26% dec^{-1}) , China (24% dec^{-1})

Chen *et al*. (2019), *Nat. Sustain.*

Net leaf area change ranked by country during 2000-2017

- China accounts for 25% of the global net increase in leaf area with only 6.6% of global vegetated area

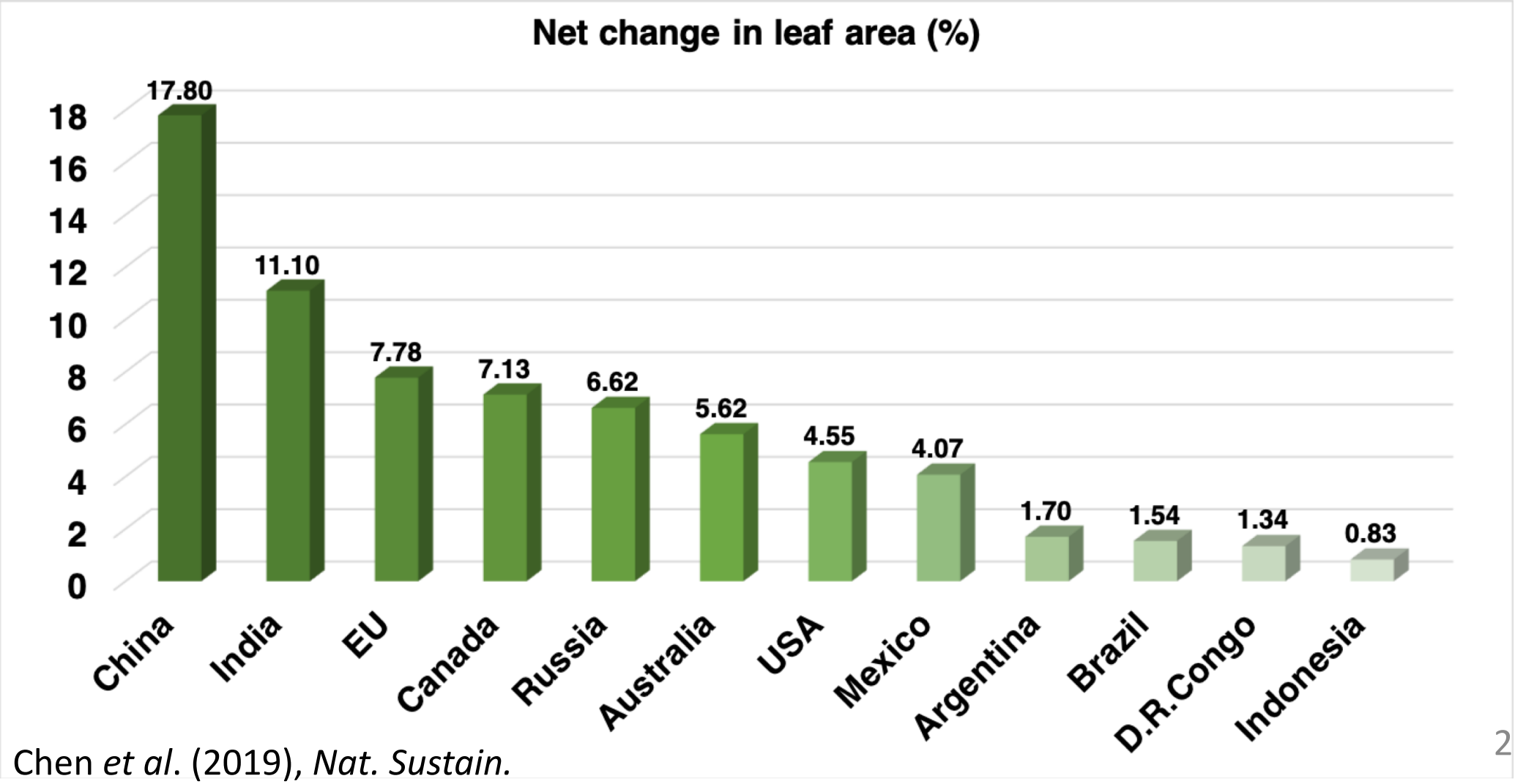

Chen *et al*. (2019), *Nat. Sustain.*

How does vegetation change impact surface temperatures?

Terminologies

- Land surface temperature (LST or $\boldsymbol{T_s}$): the radiometric skin temperature
- Near-surface air temperature ($\boldsymbol{T_{2m}}$): measured 2-m above the ground surface
- Forcing air temperature ($\boldsymbol{T_a}$) to land surface models: about 30 m above the land surface
  - ✓ In land-only models, assume the forcing air temperature does not respond to land surface changes.

Statistical method

Multivariate linear regression

- $\Delta LST = a*\Delta LAI + b*\Delta Precipitation + c * \Delta SW_{in} + d$
- Coefficient/slope *a* is the sensitivity of LST to LAI
- Not considering the global warming in air temperature e.g., due to elevated [CO_2]

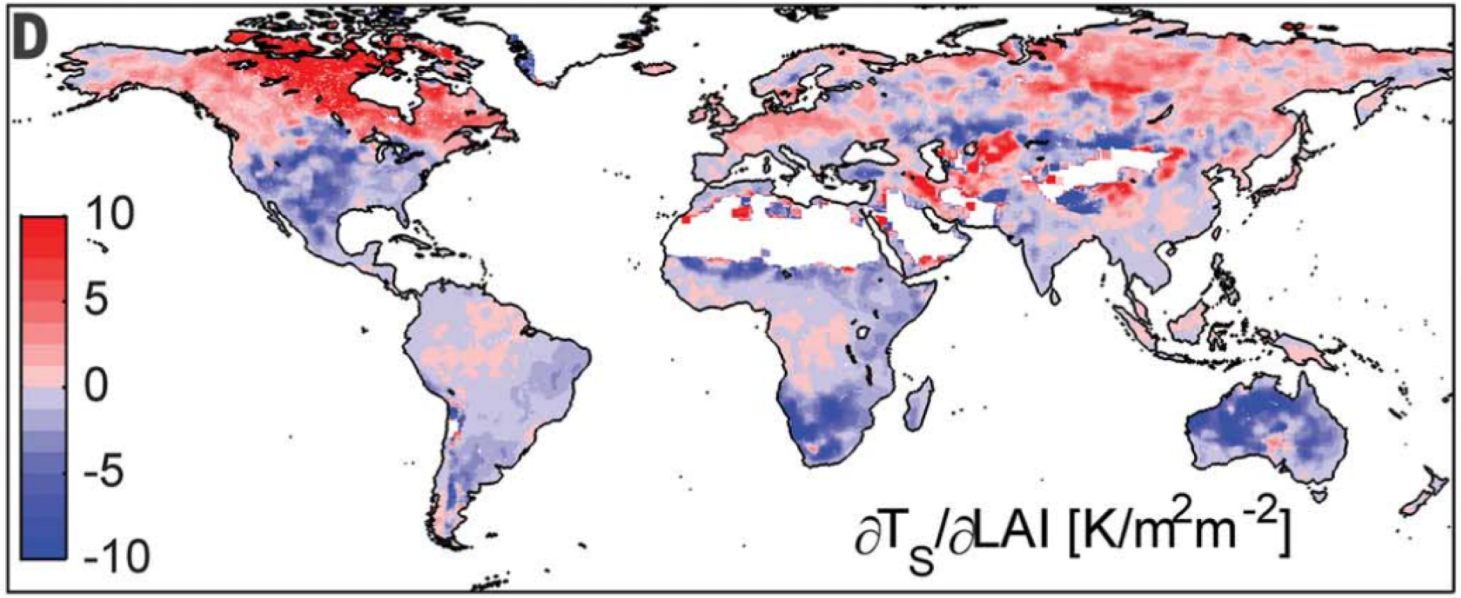

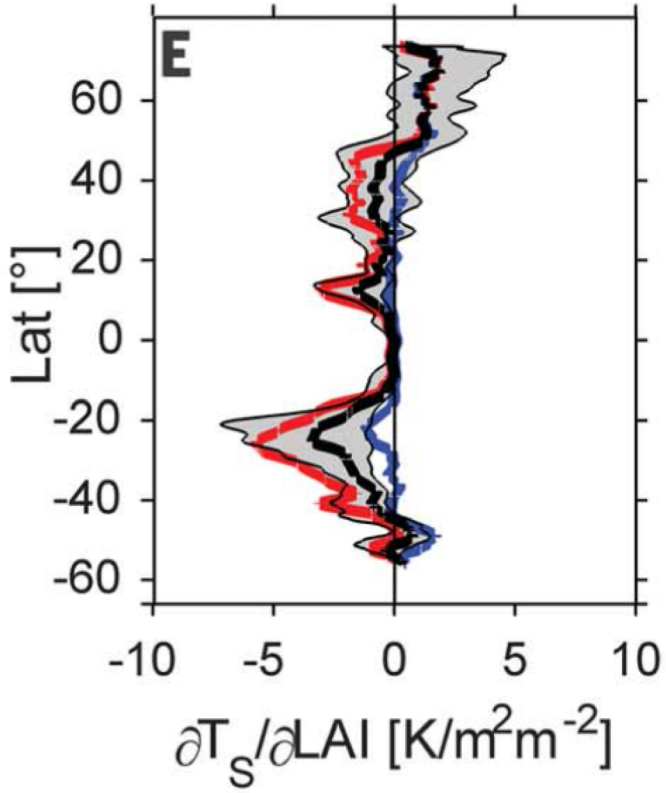

Caveat: causal ambiguity

Forzieri et al. (2017), *Science*

Comment on Forzieri et al. (2017)

Comment on "Satellites reveal contrasting responses of regional climate to the widespread greening of Earth"

Yue Li[1], Zhenzhong Zeng[1,2]*, Ling Huang[1], Xu Lian[1], Shilong Piao[1,3,4]

Forzieri *et al*. (Reports, 16 June 2017, p. 1180) used satellite data to show that boreal greening caused regional warming. We show that this positive sensitivity of temperature to the greening can be derived from the positive response of vegetation to boreal warming, which indicates that results from a statistical regression with satellite data should be carefully interpreted.

Li et al. (2018), *Science*

Comment on Forzieri et al. (2017)

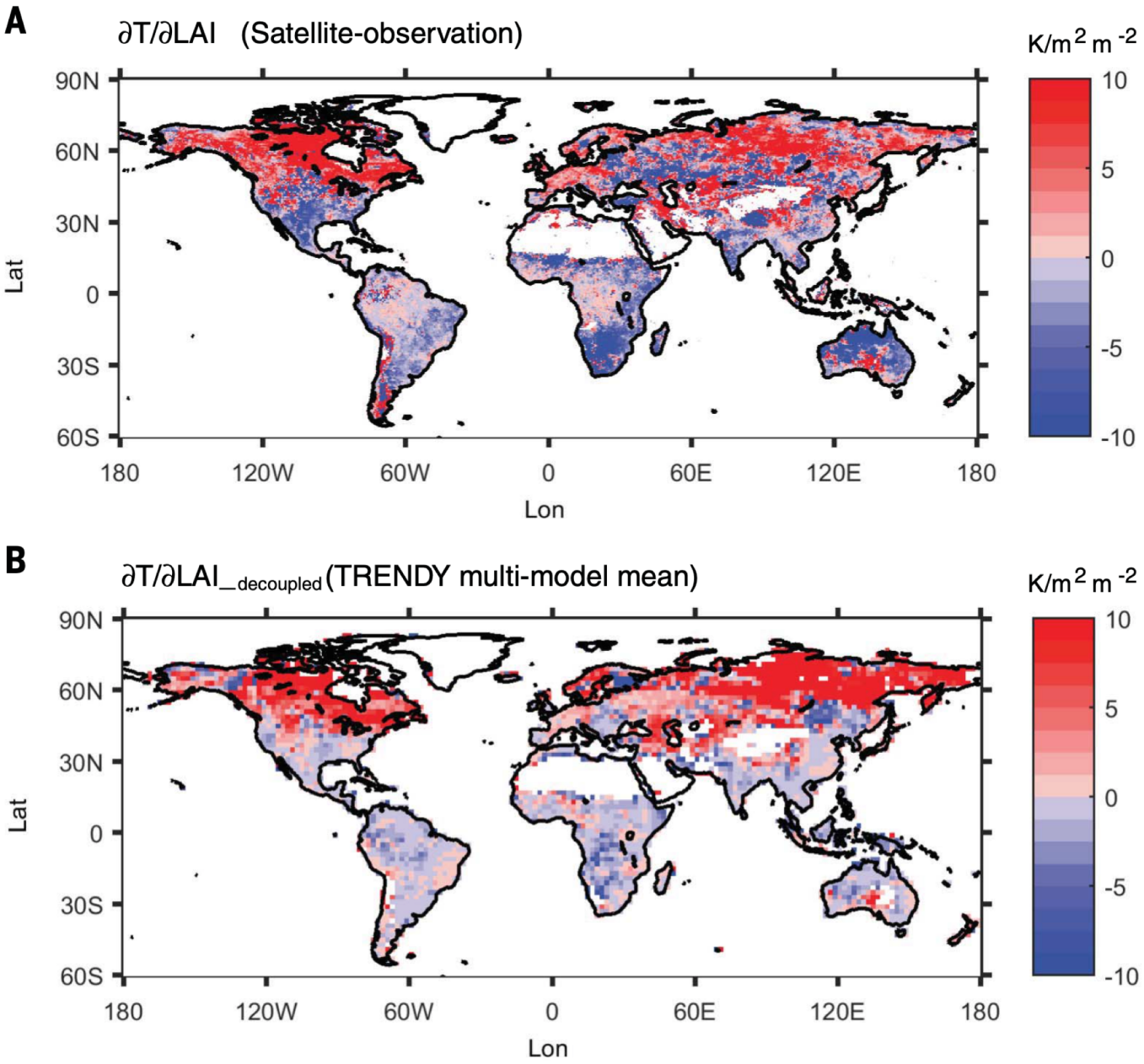

The authors almost reproduced Forzieri et al's results using multivariate linear regression

In the TRENDY models, only vegetation responds to forcing air temperature.

Show similar sensitivities in $\partial T_{2m}/\partial$LAI.

Li et al. (2018), *Science*

Response to comment on Forzieri et al. (2017)

Response to Comment on "Satellites reveal contrasting responses of regional climate to the widespread greening of Earth"

Giovanni Forzieri[1]*, Ramdane Alkama[1], Diego G. Miralles[2], Alessandro Cescatti[1]

Li *et al*. contest the idea that vegetation greening has contributed to boreal warming and argue that the sensitivity of temperature to leaf area index (LAI) is instead likely driven by the climate impact on vegetation. We provide additional evidence that the LAI-climate interplay is indeed largely driven by the vegetation impact on temperature and not vice versa, thus corroborating our original conclusions.

Authors pointed out that Li et al's comments are solely based on model simulations, and models are very uncertain and poor at simulating LAI, growing season, snow (albedo), etc.

Forzieri et al. (2018), *Science*

Response to comment on Forzieri et al. (2017)

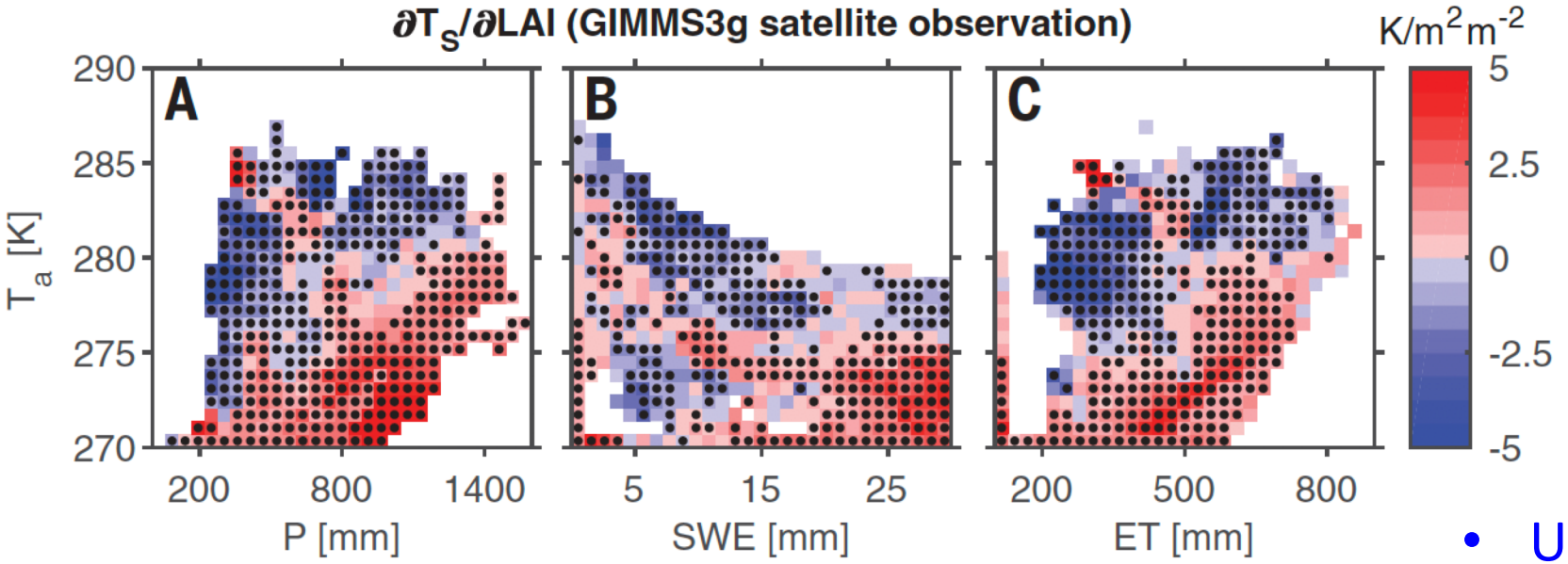

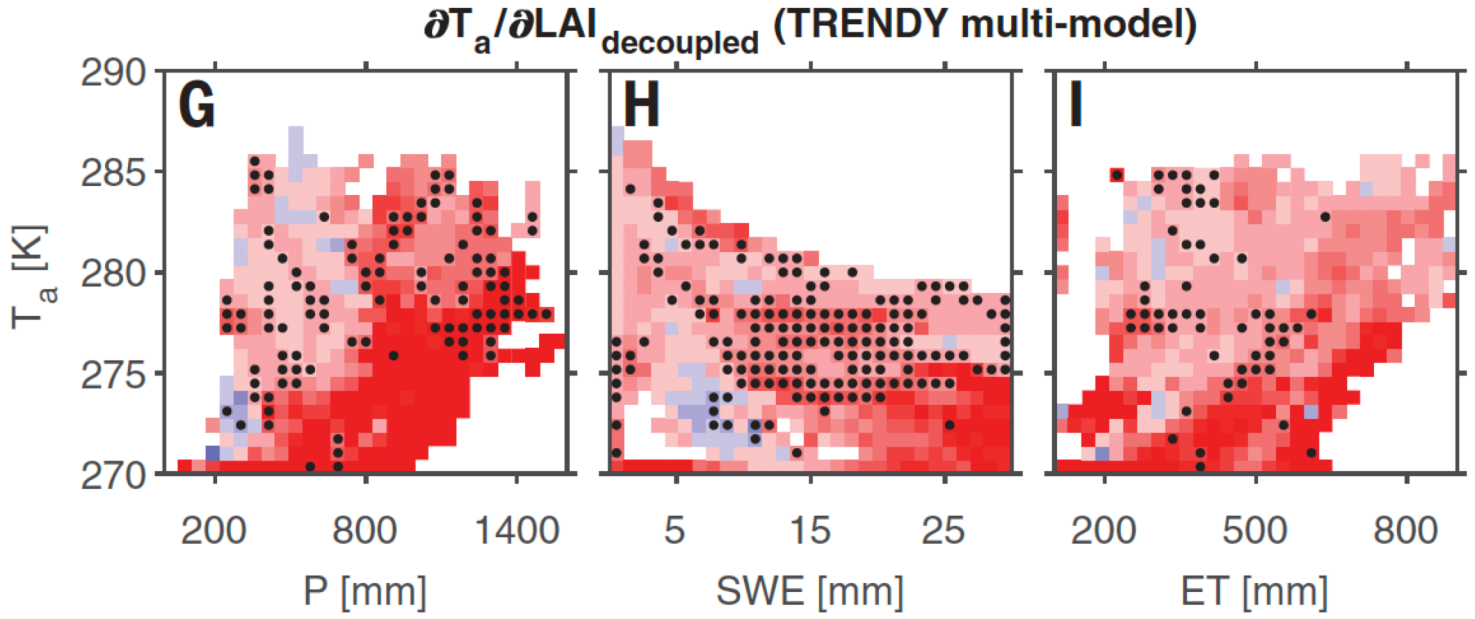

- Unclear their use of air temperatures
- TRENDY models are land only models and their forcing air temperature should not respond to land surface

Forzieri et al. (2018), *Science*

Model and observation

"We agree with Li et al. that future studies based on the integration of models and observations are required to reconcile these findings and derive conclusive statements about the climate effects of the widespread greening of Earth." - Forzieri et al. (2018), *Science*

We conducted a study that drew on the respective strengths of observations and models. See Chen et al, 2020, *Science Advances*.

Biophysical impacts of Earth greening largely controlled by aerodynamic resistance

Chi Chen[1]*, Dan Li[1]*, Yue Li[2], Shilong Piao[2], Xuhui Wang[2], Maoyi Huang[3], Pierre Gentine[4], Ramakrishna R. Nemani[5], Ranga B. Myneni[1]

Satellite observations show widespread increasing trends of leaf area index (LAI), known as the Earth greening. However, the biophysical impacts of this greening on land surface temperature (LST) remain unclear. Here, we quantify the biophysical impacts of Earth greening on LST from 2000 to 2014 and disentangle the contributions of different factors using a physically based attribution model. We find that 93% of the global vegetated area shows negative sensitivity of LST to LAI increase at the annual scale, especially for semiarid woody vegetation. Further considering the LAI trends ($P \leq 0.1$), 30% of the global vegetated area is cooled by these trends and 5% is warmed. Aerodynamic resistance is the dominant factor in controlling Earth greening's biophysical impacts: The increase in LAI produces a decrease in aerodynamic resistance, thereby favoring increased turbulent heat transfer between the land and the atmosphere, especially latent heat flux.

Schematic of LST and energy balance

Governing equation

$$S_{in}(1-\alpha) + \varepsilon L_{in} - \varepsilon\sigma T_s^{\,4} = H + LE + G$$

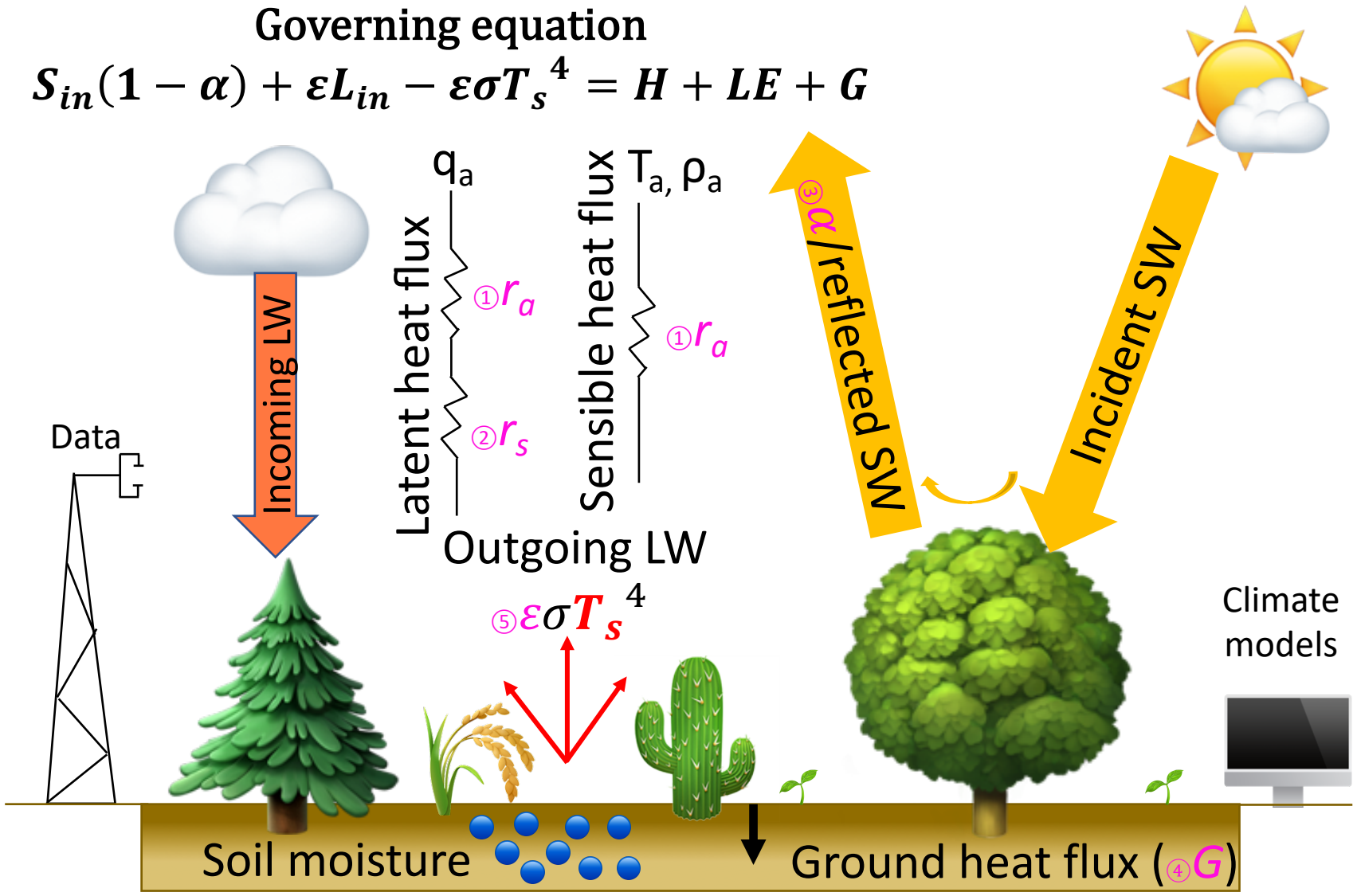

Mechanisms affect LST

$$S_{in}(1-\alpha)+\varepsilon L_{in}-\epsilon\sigma T_s^4=\frac{\rho c_p}{r_a}(T_s-T_a)+\frac{\rho L_v}{r_a+r_s}[q_s^*(T_s)-q_a]+G$$

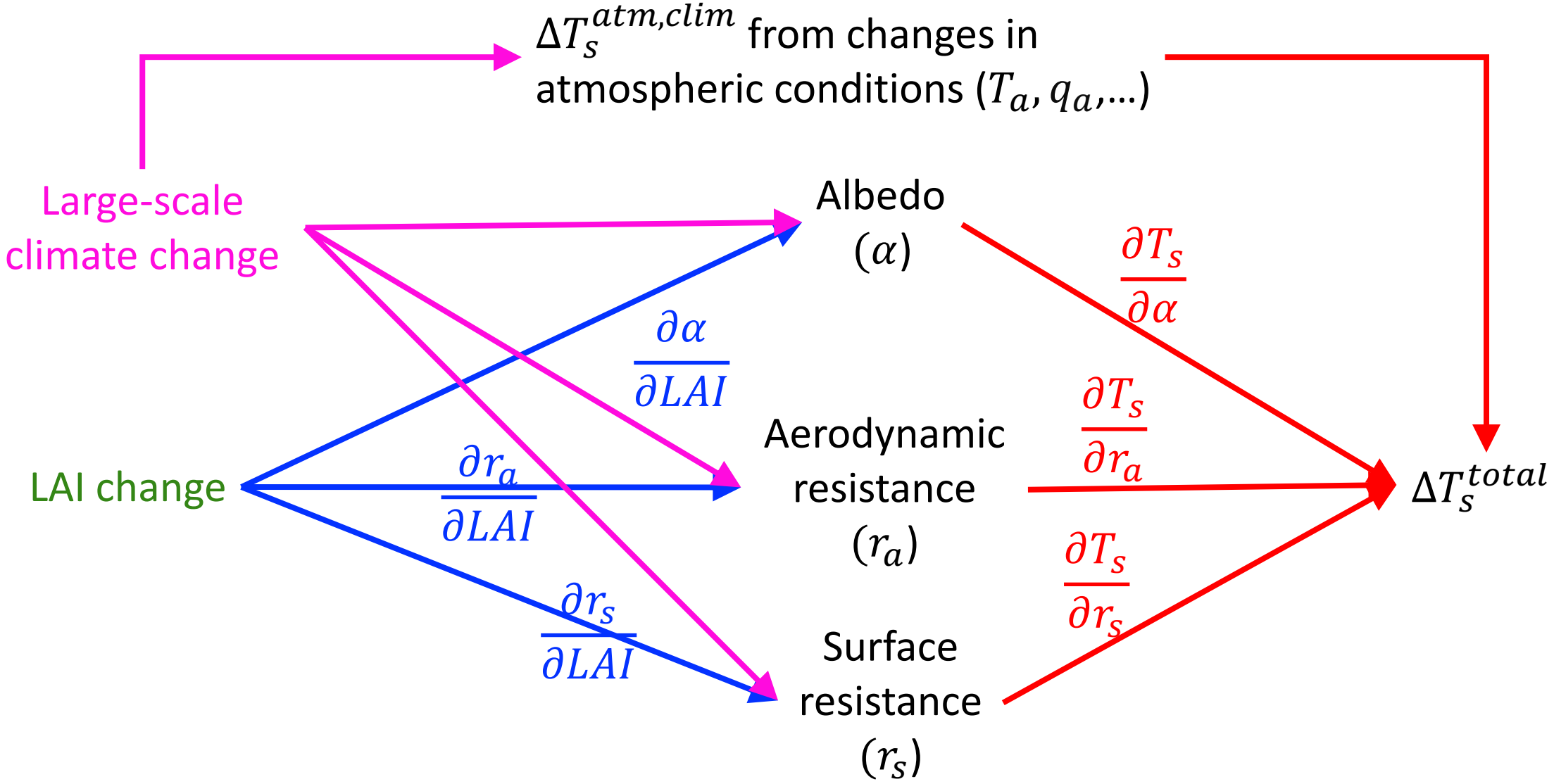

ΔT_s: Two resistance mechanism

❑ Analytical expression of T_s 「Two resistance mechanism, TRM, Rigden and Li (2017), *GRL*」

$$T_s = \frac{S_{in}(1-\alpha) + \varepsilon L_{in} - \varepsilon\sigma {T_a}^4 - G - \frac{\rho L_v}{(r_a + r_s)}(q_a^*(T_a) - q_a)}{4\varepsilon\sigma {T_a}^3 (1+f)} + T_a$$

❑ The change of LST due to changes in biophysical factors induced by LAI change

$$\Delta T_s^{bio,LAI} = \frac{\partial T_s^{bio}}{\partial LAI}\Delta LAI_{sat} = \left[\left(\frac{\partial T_s}{\partial \alpha}\right)\left(\frac{\partial \alpha}{\partial LAI}\right) + \left(\frac{\partial T_s}{\partial r_a}\right)\left(\frac{\partial r_a}{\partial LAI}\right) + \left(\frac{\partial T_s}{\partial r_s}\right)\left(\frac{\partial r_s}{\partial LAI}\right) + \ \ldots\right] \times \Delta LAI_{sat}$$

CLM5 simulations

Analytically computed

MODIS LAI

The TRM method can solve T_s and its change.

Sensitivity of LST to LAI by different methods

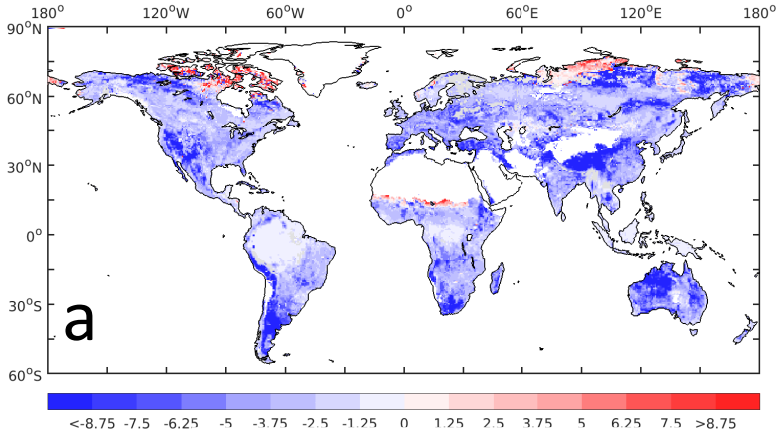

$$\frac{\partial T_s^{bio}}{\partial LAI}(10^{-1}\ K\ m^2\ m^{-2})$$

CLM5 TRM (main result)

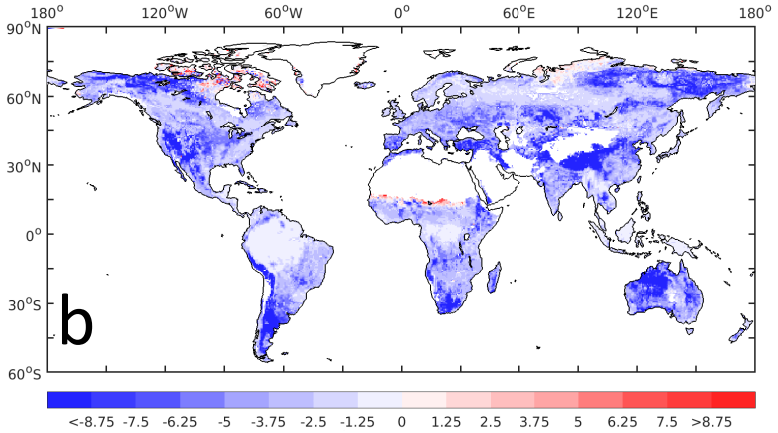

$$\frac{\Delta T_s}{\Delta LAI}(10^{-1}\ K\ m^2\ m^{-2})$$

CLM5 sensitivity experiments

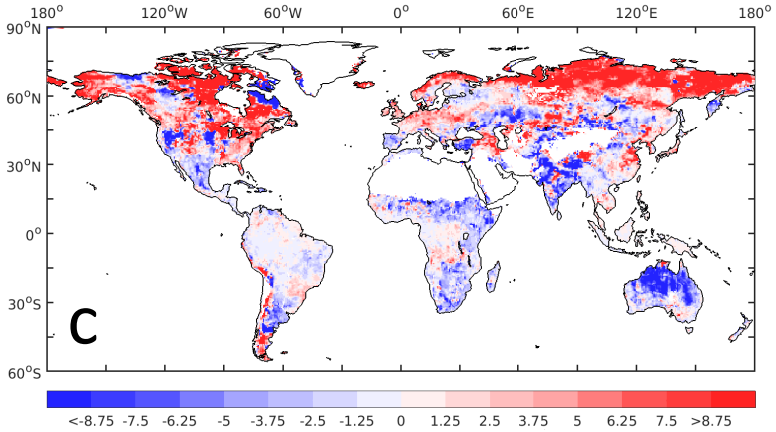

$$\frac{\partial T_s^{reg}}{\partial LAI}(m^2\ m^{-2})$$

CLM5 regression

- Sensitivity diagnosed by TRM method (*Fig a*) is consistent with CLM5 sensitivity experiments (*Fig b*);
- Sensitivity derived by the multiple regression method (*Fig c*) is **NOT** consistent with CLM5 sensitivity experiments (*Fig b*) .

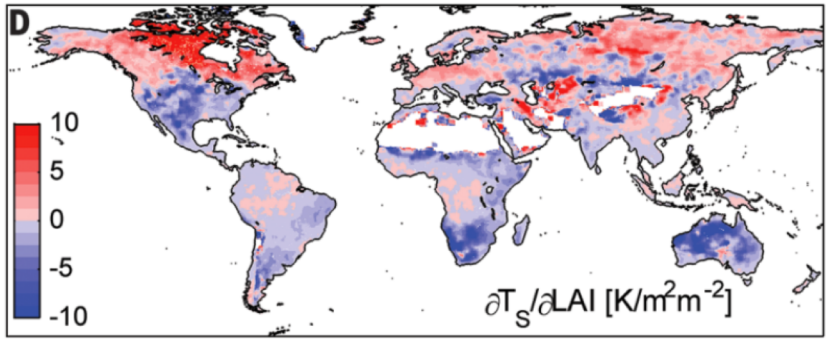

Forzieri et al. (2017)

LST and air temperature

Sensitivity of LST to air temperature

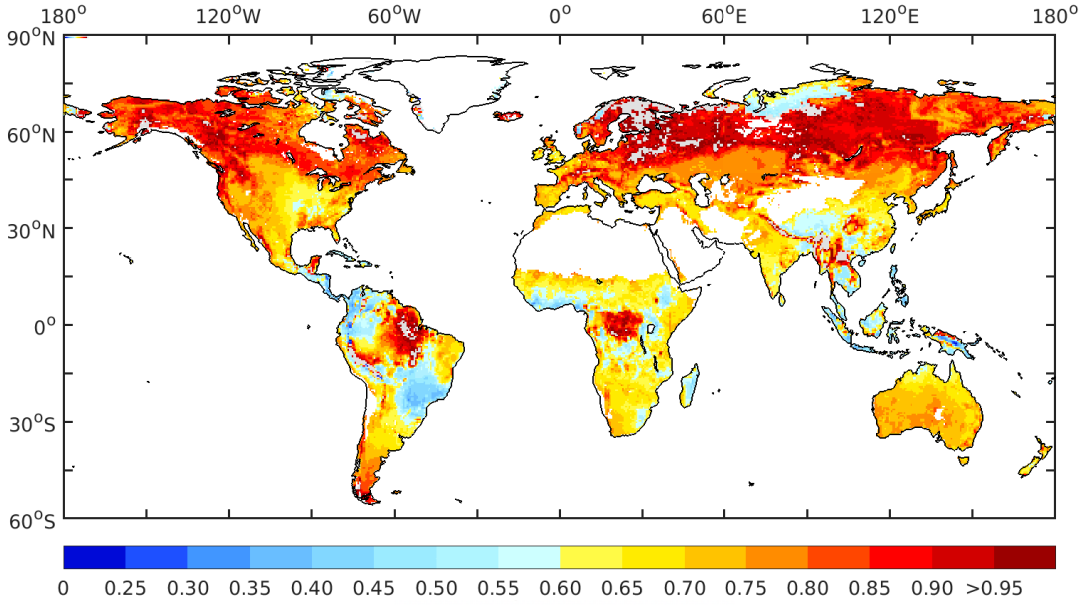

$$\frac{\partial T_s}{\partial T_a}(K\ K^{-1})$$

Sensitivity of LST to LAI estimated by the multiple regression method with air temperature included

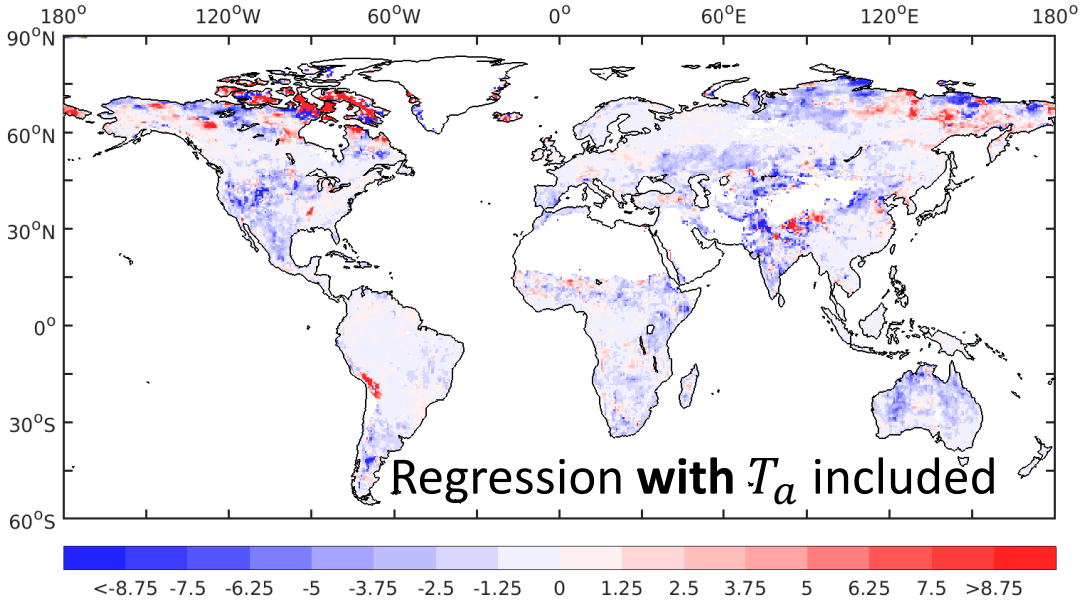

$$\frac{\partial T_s^{reg}}{\partial LAI}(m^2\ m^{-2})$$

Results from multiple regression are quite uncertain.

Sensitivity of LST to LAI by different inputs

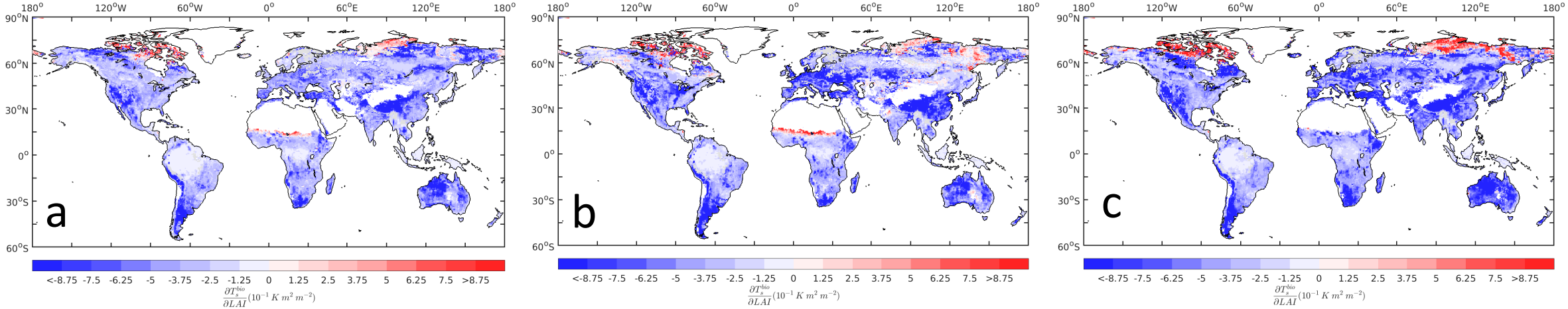

e.g., $\frac{\partial T_s}{\partial \alpha}$ e.g., $\frac{\partial \alpha}{\partial LAI}$

CLM5 TRM (main result)

MERRA-2 + CLM5 TRM

e.g., $\frac{\partial T_s}{\partial \alpha}$ e.g., $\frac{\partial \alpha}{\partial LAI}$

MMEM + CLM5 TRM

e.g., $\frac{\partial T_s}{\partial \alpha}$ e.g., $\frac{\partial \alpha}{\partial LAI}$

- Sensitivity diagnosed from CLM5 outputs (*Fig. a*) is consistent with that diagnosed from a combination of CLM5 and MERRA-2 (*Fig. b*) or a combination of CLM5 and CMIP5 (*Fig. c*) .

Sensitivity of LST to LAI

Table 1. Mean and SD of the biophysical sensitivity of LST to LAI across bioclimatic regimes. Mean ± 1 SD, where SD indicates the spatial variability. OWV, other woody vegetation.

	Forests	OWV	Grasslands	Croplands	All vegetation
Global	−0.23 ± 0.12	−0.45 ± 0.32	−0.36 ± 0.23	−0.43 ± 0.17	−0.36 ± 0.22
By latitude					
>50°S/N	−0.28 ± 0.09	−0.37 ± 0.36	−0.07 ± 0.52	−0.44 ± 0.16	−0.34 ± 0.23
25°S/N–50°S/N	−0.26 ± 0.09	−0.58 ± 0.29	−0.47 ± 0.31	−0.45 ± 0.15	−0.44 ± 0.23
25°S–25°N	−0.11 ± 0.05	−0.45 ± 0.23	−0.33 ± 0.13	−0.37 ± 0.18	−0.29 ± 0.19
By LAI					
LAI < 1 m^2 m^{-2}	−0.38 ± 0.15	−0.49 ± 0.38	−0.37 ± 0.37	−0.46 ± 0.17	−0.45 ± 0.31
LAI ∈1–4 m^2 m^{-2}	−0.25 ± 0.08	−0.33 ± 0.11	−0.33 ± 0.11	−0.39 ± 0.14	−0.30 ± 0.11
LAI > 4 m^2 m^{-2}	−0.09 ± 0.02	−0.13 ± 0.03	−0.12 ± 0.02	−0.11 ± 0.02	−0.09 ± 0.02
By annual total precipitation (ATP)					
ATP < 900 mm	−0.29 ± 0.09	−0.47 ± 0.36	−0.35 ± 0.30	−0.43 ± 0.17	−0.40 ± 0.26
ATP ∈ 900–2000 mm	−0.21 ± 0.10	−0.35 ± 0.13	−0.37 ± 0.15	−0.43 ± 0.16	−0.33 ± 0.16
ATP > 2000 mm	−0.10 ± 0.04	−0.31 ± 0.17	−0.31 ± 0.19	−0.33 ± 0.18	−0.12 ± 0.06

The dominant role of aerodynamic resistance

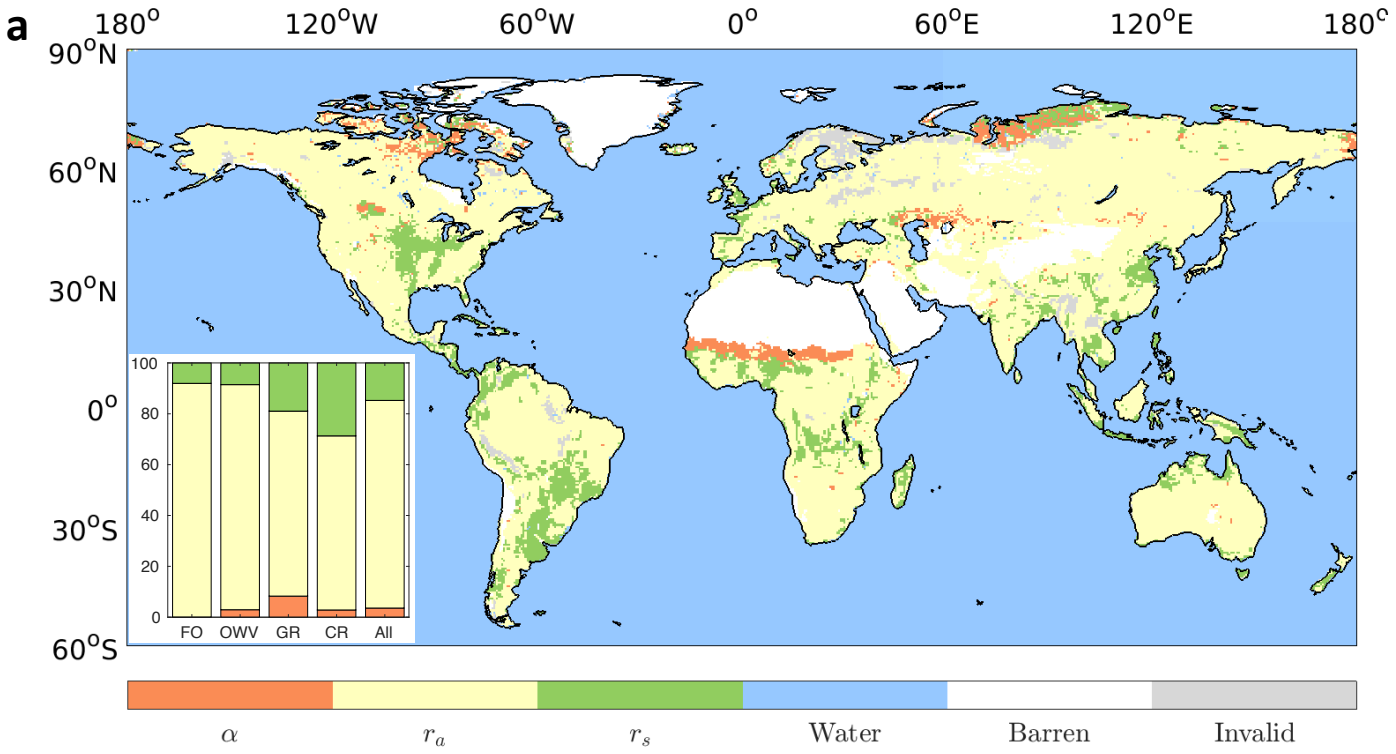

a. Dominant surface biophysical factors in regulating $\partial T_S^{bio}/\partial LAI$.

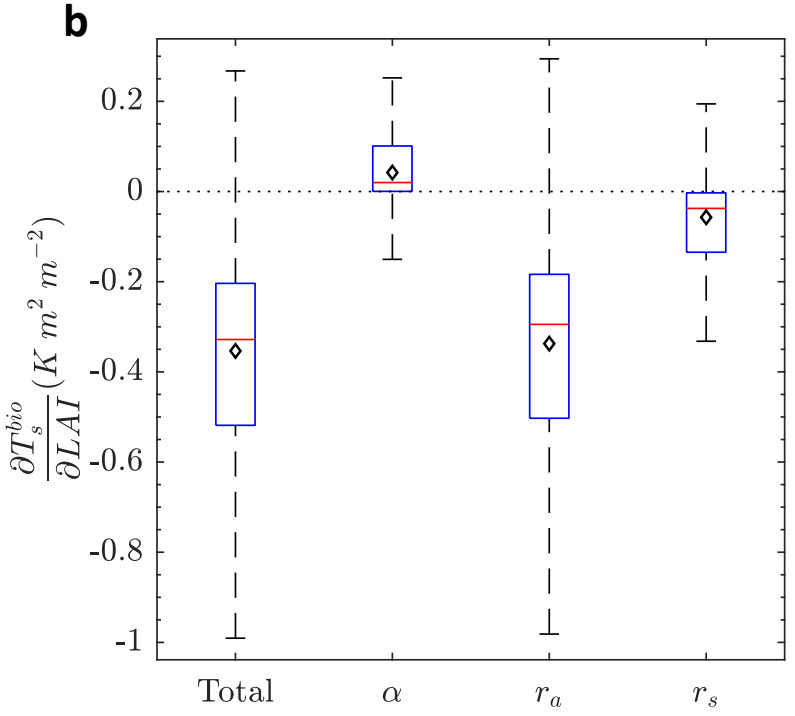

b. Attribution of $\frac{\partial T_S^{bio}}{\partial LAI}$ with surface biophysical factors.

- r_a dominates 82% of the vegetated area (Fig a)
- r_a contributes most of the cooling signal (Fig b)
  - ➢ LAI increase → rougher → r_a ↓ → LE↑ or H↑, especially the LE

Turbulent flux sensitivity

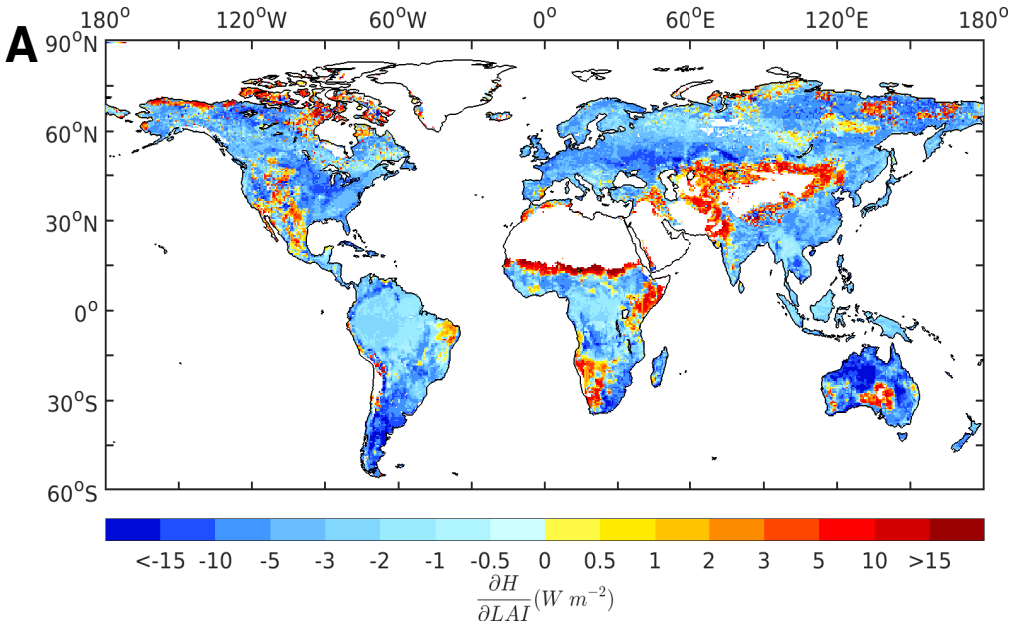

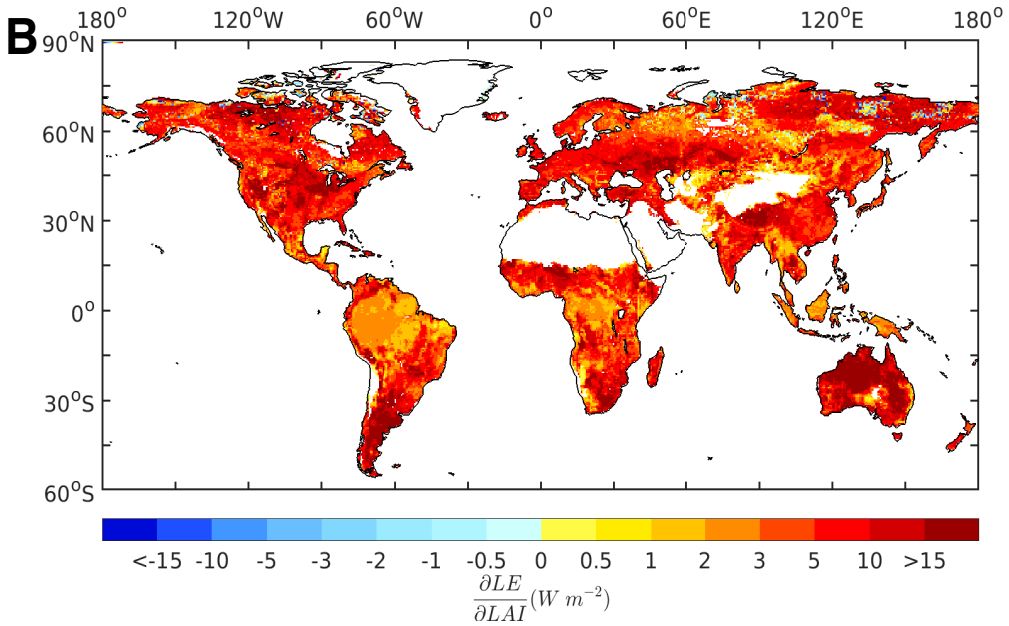

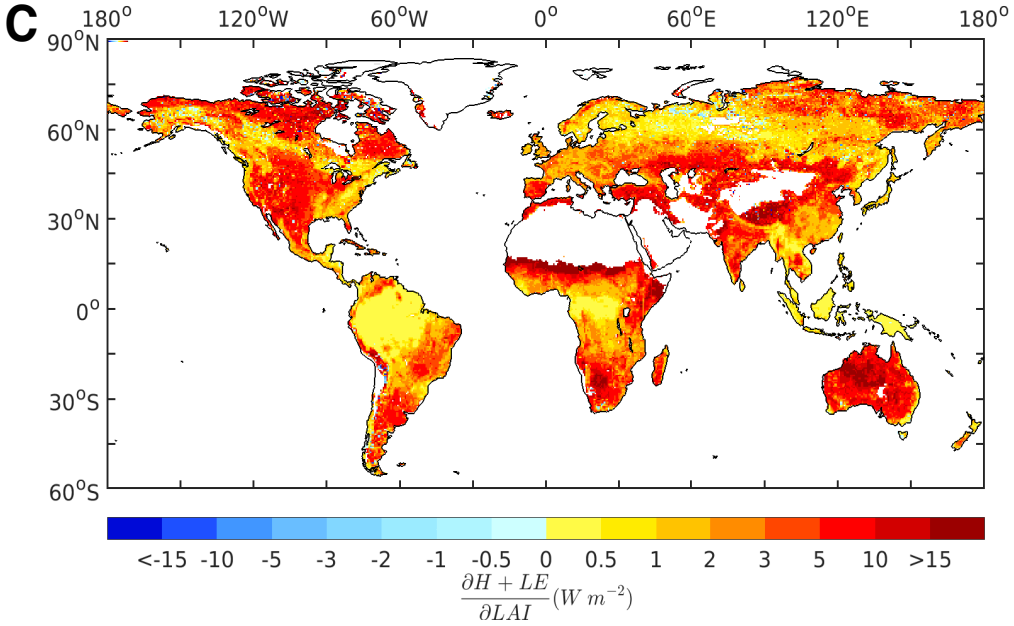

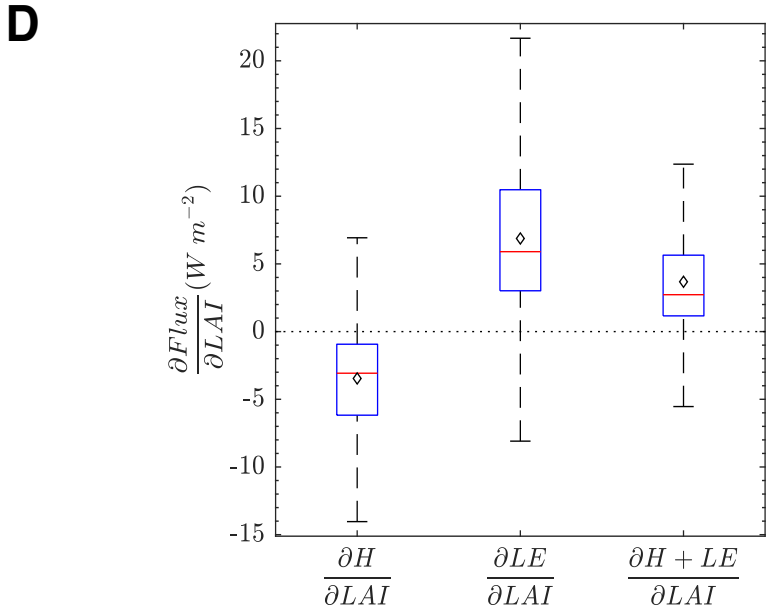

Change of LST due to greening

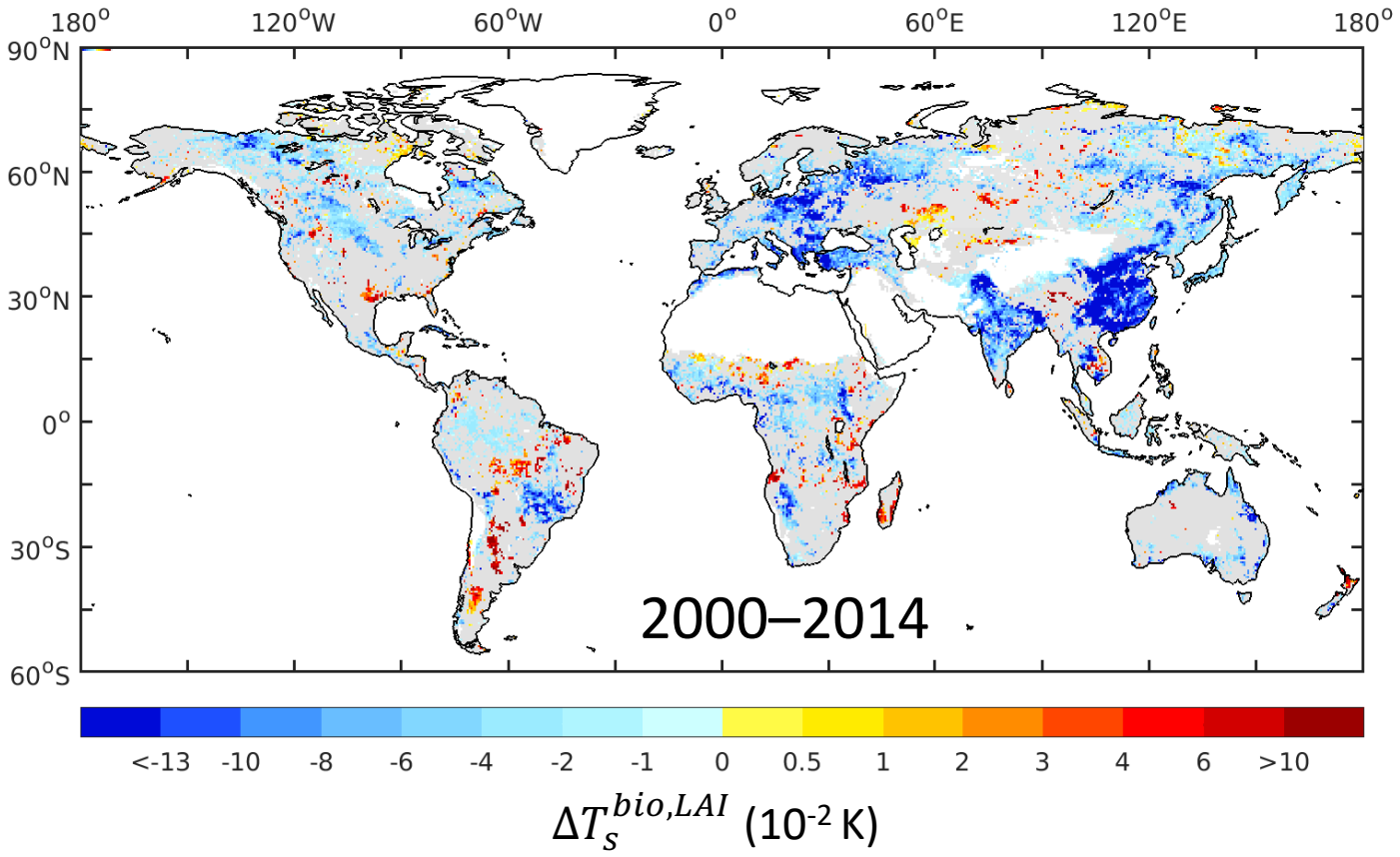

- $\Delta T_s^{bio,LAI} = \frac{\partial T_s^{bio}}{\partial LAI} \times \Delta LAI_{sat}$

Cooling caused by LAI change (2000~2014) = -2.97 ×10^{21} joules, which is:

- 5 times of world total primary energy supply in 2015, International Energy Agency, (2017)
- 25 times of the warming caused by land cover change (2000~2015), Duveiller et al., (2018) *NC*

Changes in vegetation over urban areas (summer time)

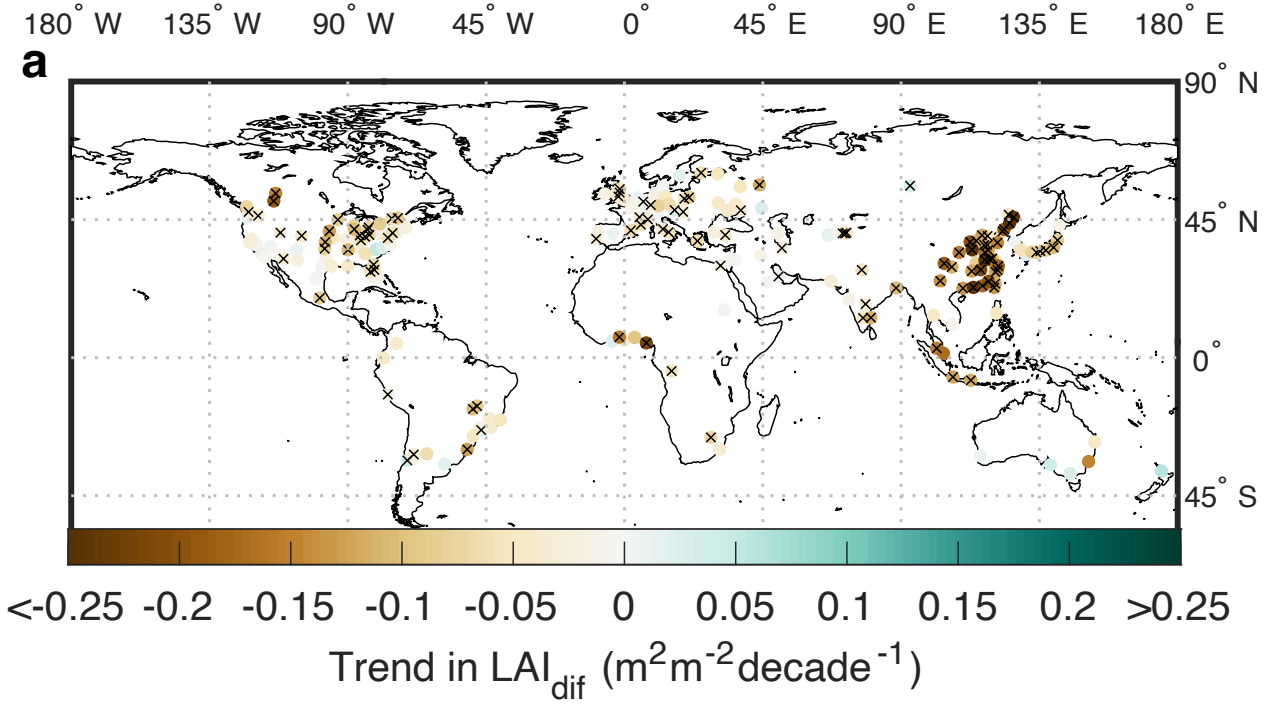

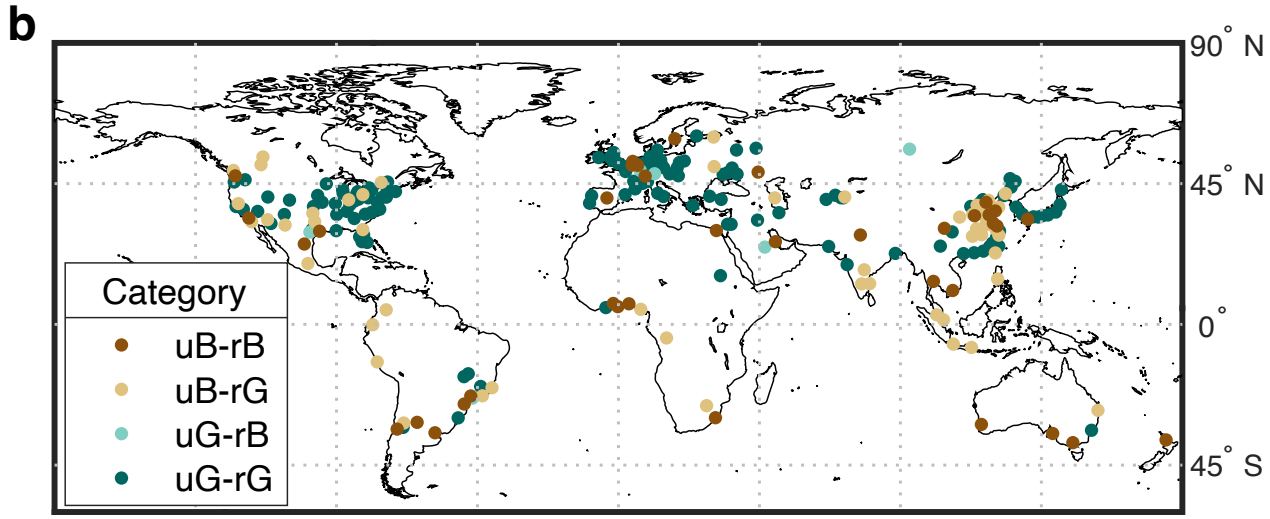

Chen *et al.* (2021) *ERL*

- 228 megacities in total
- 189 (39) show a decreasing (increasing) trend of LAI_{dif}
- uG-rG: 133 (better env.)
- uB-rG: 52 (stronger contrast)
- uB-rB: 43 (strong urbanization)
- uG-rB: 6 (possible recession or suburbanization)

Changes in urban heat island (summer time)

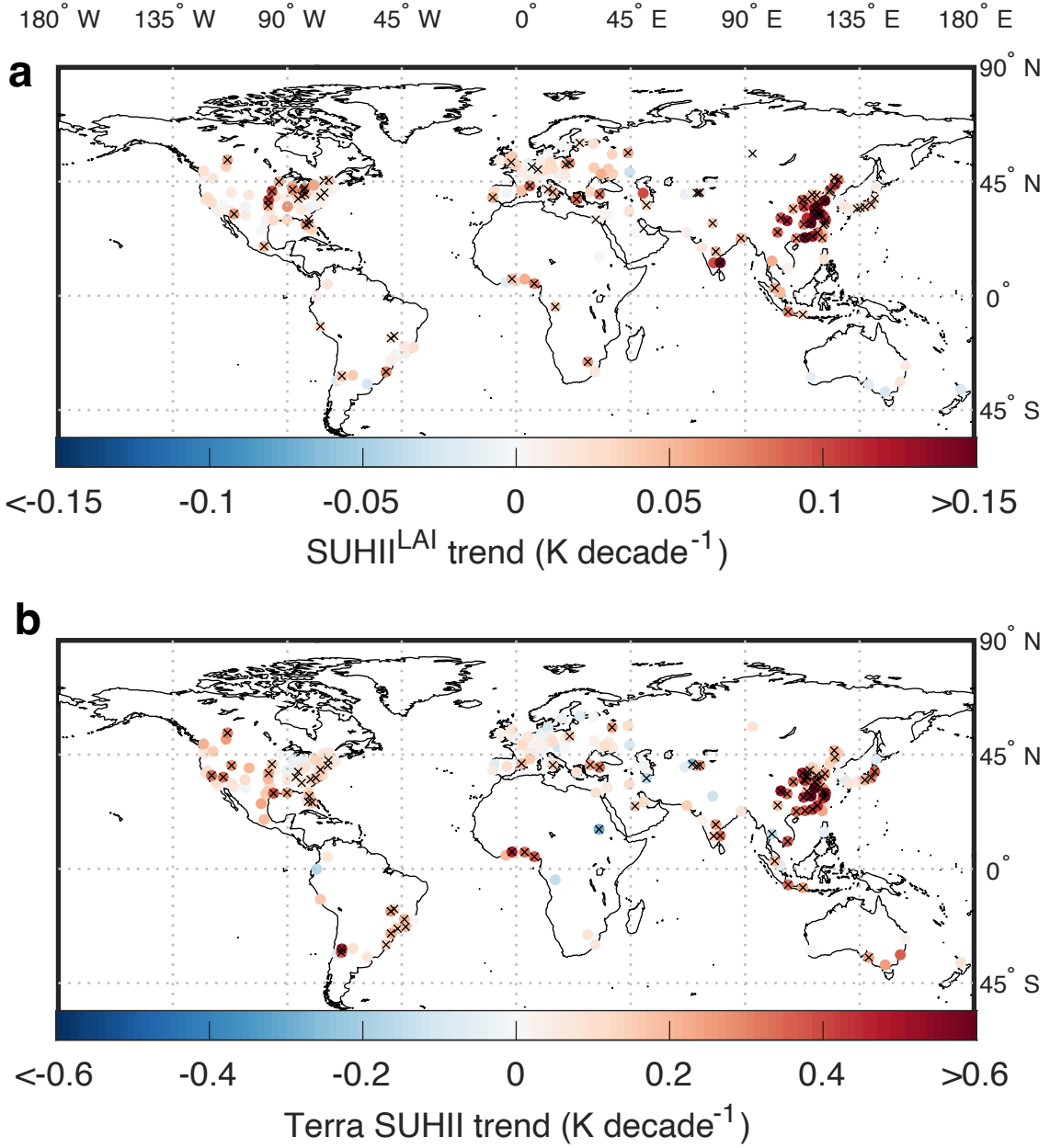

Chen *et al.* (2021) *ERL*

- Hefei (China) and Chennai (India) rank 1st and 2nd in terms of $\Delta SUHII^{LAI}$ (0.29 and 0.28 K decade^{-1})
- Vegetation biophysical effect ($\Delta SUHII^{LAI}$) on average contribute 25% of the trend in total SUHII trend "observed" by Terra MODIS

Sensitivity of urban heat island to LAI change

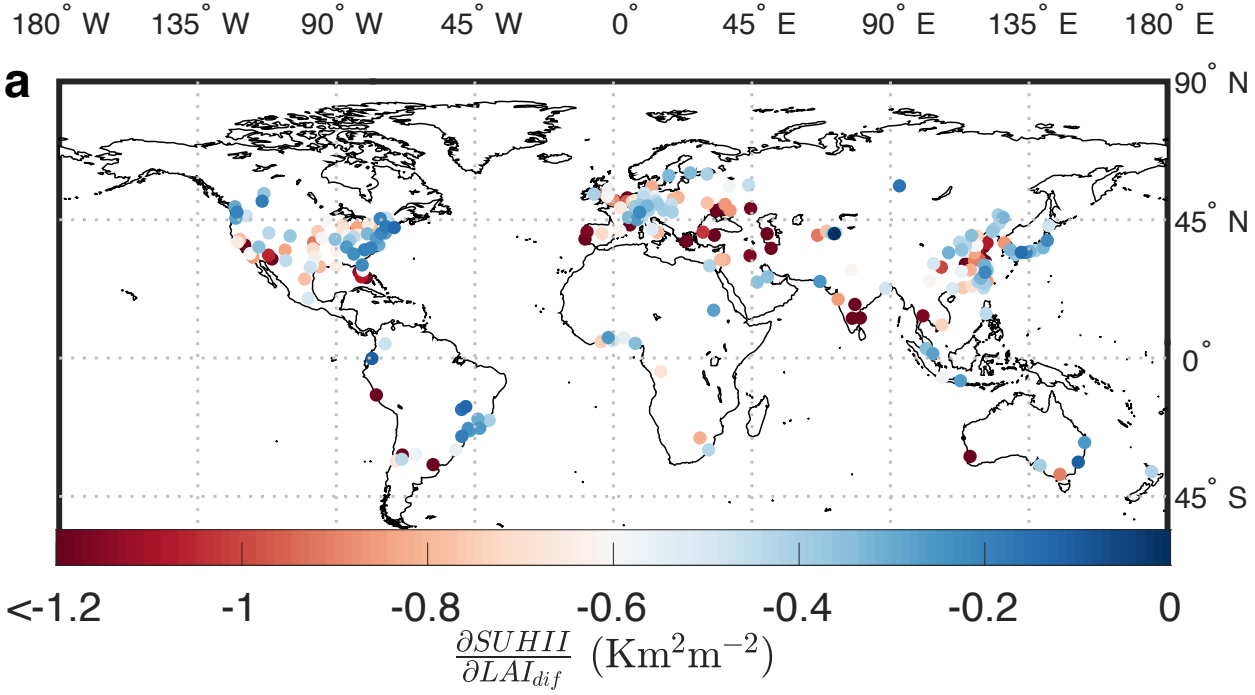

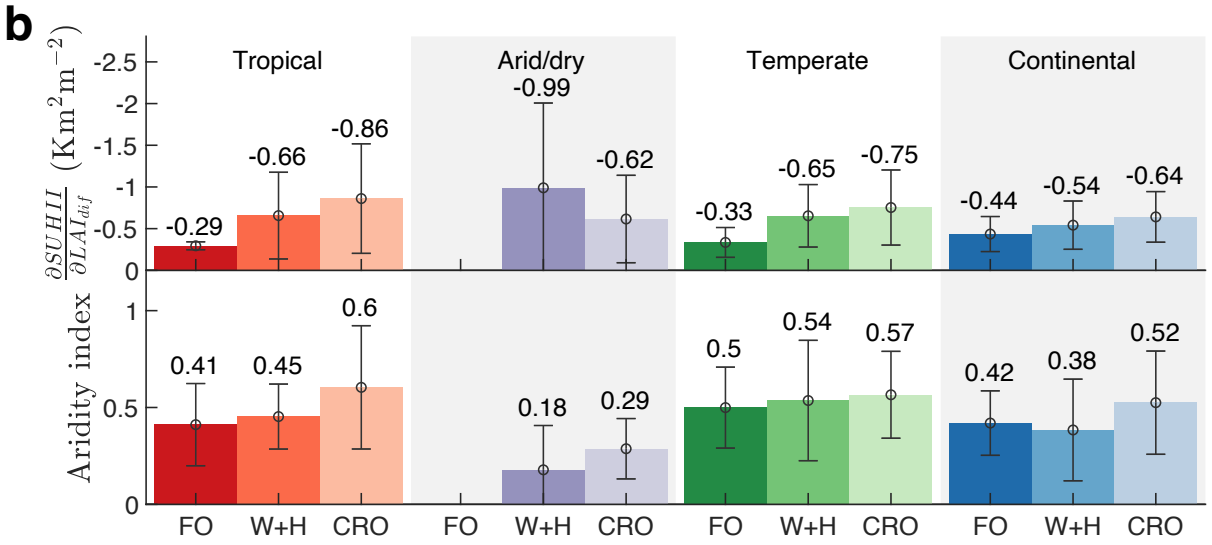

Chen *et al.* (2021) *ERL*

- Strong spatial difference in $\frac{\partial SUHII}{\partial LAI}$
- Shaped by biome type and aridity
- Aridity index = precip. / potential ET
  - Higher aridity index means a wetter climate
- SUHII is more sensitive to LAI change in cropland-surrounding (CRO) cities than forest-surrounding (FO) cities

Dominate factor of the sensitivity of urban heat island

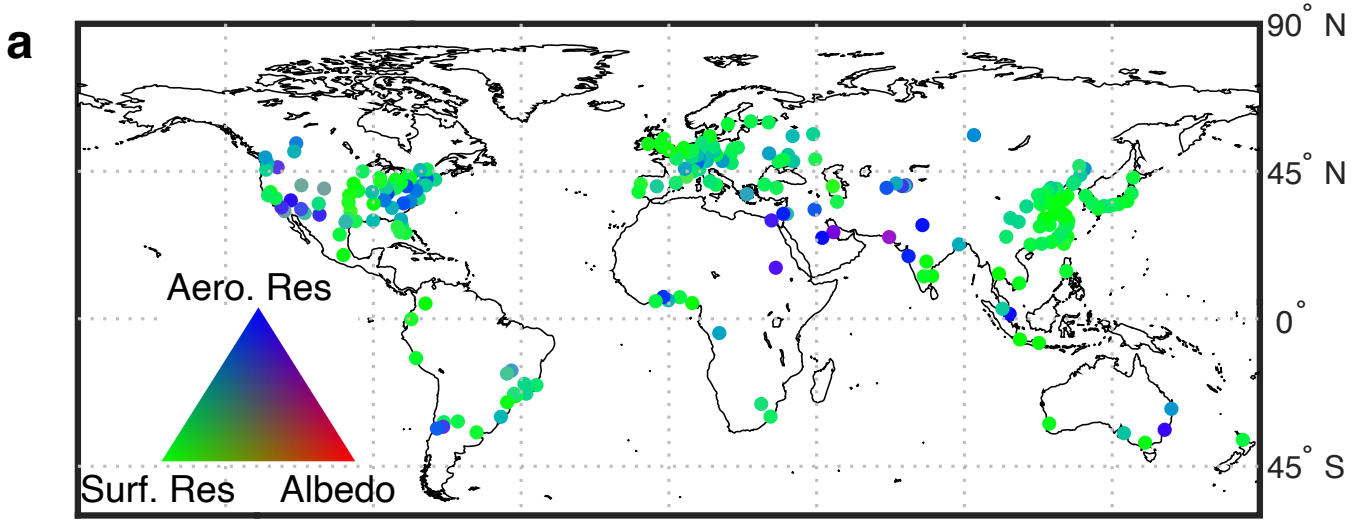

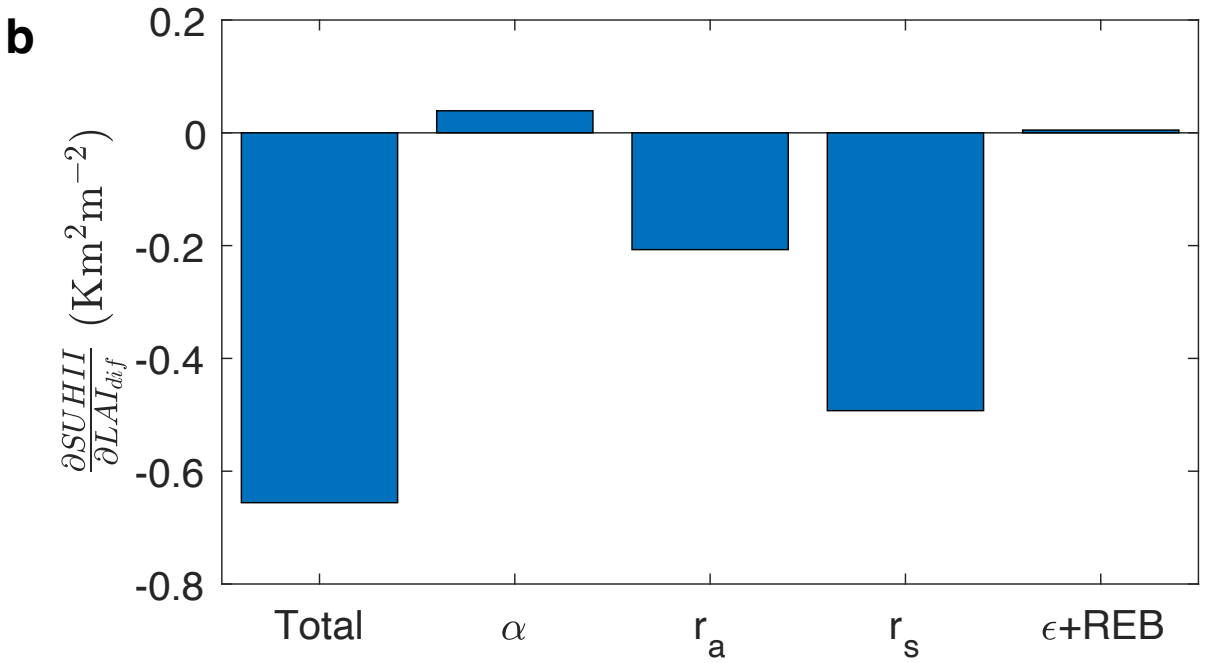

Chen *et al.* (2021) *ERL*

- Previous study shows that temperature change is dominated by the aerodynamic resistance (r_a) pathway for remote vegetation (Chen *et al.* 2020).
- Here, SUHII is dominated by the surface resistance (r_s) pathway in the "urban-rural" system, emphasizing the important role of perviousness (for water) of the surface.

Thank you!